Lanthanide(III) Complexes of Novel Mixed Carboxylic-Phosphorus Acid Derivatives of Diethylenetriamine: A Step towards More Efficient MRI Contrast Agents

Jan Kotek,[a, b] Petra Lebdušková,[a, b] Petr Hermann,[b] Luce Vander Elst,[c] Robert N. Muller,[c] Carlos F. G. C. Geraldes,[d] Thomas Maschmeyer,[a] Ivan Lukeš,*[b] and Joop A. Peters*[a]

Abstract: Three novel phosphorus-containing analogues of H_5DTPA (DTPA = diethylenetriaminepentaacetate) were synthesised (H_6L^1, H_5L^2, H_5L^3). These compounds have a -CH_2-P(O)(OH)-R function (R = OH, Ph, CH_2NBn_2) attached to the central nitrogen atom of the diethylenetriamine backbone. An NMR study reveals that these ligands bind to lanthanide(III) ions in an octadentate fashion through the three nitrogen atoms, a P–O oxygen atom and four carboxylate oxygen atoms. The complexed ligand occurs in several enantiomeric forms due to the chirality of the central nitrogen atom and the phosphorus atom upon coordination. All lanthanide complexes studied have one coordinated water molecule. The residence times (τ_M^{298}) of the coordinated water molecules in the gadolinium(III) complexes of H_6L^1 and H_5L^2 are 88 and 92 ns, respectively, which are close to the optimum. This is particularly important upon covalent and noncovalent attachment of these Gd^{3+} chelates to polymers. The relaxivity of the complexes studied is further enhanced by the presence of at least two water molecules in the second coordination sphere of the Gd^{3+} ion, which are probably bound to the phosphonate/phosphinate moiety by hydrogen bonds. The complex $[Gd(L^3)(H_2O)]^{2-}$ shows strong binding ability to HSA, and the adduct has a relaxivity comparable to MS-325 ($40\ s^{-1}mM^{-1}$ at 40 MHz, 37 °C) even though it has a less favourable τ_M value (685 ns). Transmetallation experiments with Zn^{2+} indicate that the complexes have a kinetic stability that is comparable to—or better than—those of $[Gd(dtpa)(H_2O)]^{2-}$ and [Gd(dtpa-bma)(H_2O)].

Keywords: chelates · imaging agents · lanthanides · NMR spectroscopy · phosphinate complexes · phosphonate complexes

Introduction

Metal chelates of the polyaminocarboxylates $DTPA^{5-}$ ($DTPA^{5-}$ = diethylenetriamine-*N*,*N*,*N*′,*N*″,*N*″-pentaacetate), $DOTA^{4-}$ ($DOTA^{4-}$ = 1,4,7,10-tetraazacyclododecane-1,4,7,10-tetraacetate) and derivatives thereof have found widespread use in medical diagnosis (e.g. Magnetic Resonance Imaging, MRI; Positron Emission Tomography, PET; or Single-Photon Emission Computed Tomography, SPECT) and in radiotherapy.[1–3] These complexes have high thermodynamic and kinetic stabilities, essential features for in vivo applications, since the metal aqua ions as well as their ligands are toxic, whereas the complexes are not. The applicability of radioactive complexes also requires that complexation should be rapid enough to allow radiolabelling by a simple procedure just prior to the diagnostic procedure or the treatment. Complexes of $DTPA^{5-}$ meet this requirement, while the formation of complexes of $DOTA^{4-}$ is usually very slow.

[a] Dr. J. A. Peters, J. Kotek, P. Lebdušková, Prof. Dr. T. Maschmeyer
Laboratory for Applied Organic Chemistry and Catalysis
Delft University of Technology
Julianalaan 136, 2628 BL Delft (The Netherlands)
Fax: (+31) 152-784-289
E-mail: J.A.Peters@tnw.tudelft.nl

[b] Prof. Dr. I. Lukeš, J. Kotek, P. Lebdušková, Dr. P. Hermann
Department of Inorganic Chemistry, Charles University
Hlavova 2030, 12840 Prague (Czech Republic)
E-mail: lukes@natur.cuni.cz

[c] Prof. Dr L. Vander Elst, Prof. Dr. R. N. Muller
NMR Laboratory, Department of Organic Chemistry
University of Mons–Hainaut, 7000 Mons (Belgium)

[d] Prof. Dr. C. F. G. C. Geraldes
Departamento de Bioquímica
Faculdade de Ciências e Tecnologica, e Centro de Neurociências
Universidade de Coimbra, 3049 Coimbra (Portugal)

Supporting information for this article is available on the WWW under http://www.chemeurj.org/ or from the author.

 DOI: 10.1002/chem.200305155

MRI contrast agents are mostly Gd^{3+} complexes, as this paramagnetic ion has a relatively long electronic relaxation time, which leads to high nuclear relaxation efficiency. This is usually expressed as the relaxivity, r_1, which is the enhancement of the water proton relaxation rate in $s^{-1}mM^{-1}$. Other important parameters governing the relaxivity are the rotational correlation time (τ_R), the number of Gd^{3+}-bound water molecules (q), their residence time (τ_M) and the electron spin relaxation times (T_{ie}, $i = 1,2$). Theory predicts optimal efficiency for high-molecular-weight gadolinium(III) chelates if the residence time, τ_M, is in the range of 20–50 ns.[4] All current commercial Gd^{3+}-based contrast agents have low molecular weights and are hydrophilic. Consequently, these compounds are distributed rather unselectively over the extracellular fluids. More efficient contrast agents are being developed that may be directed to targets of interest, thereby achieving higher local concentrations at lower dosages.[5] These agents usually are conjugates of one or more Gd^{3+} chelates and a targeting vector. The criterion regarding the water exchange rate is particularly critical to achieve optimal efficiency for this new class of compounds. The current commercial Gd^{3+} chelates show water exchange rates that are an order of magnitude lower than the optimal value.[1,2,4,6] Recently, it was shown that phosphorus-containing analogues of the commercially used $[Gd(dota)(H_2O)]^-$ complex have faster water exchange than the parent system.[7] Similar results were observed on pyridine-containing macrocyclic ligands with phosphonic acid pendant arms.[8,9] Moreover, these compounds show rapid complex formation, which makes them suitable for radiodiagnostic and radiotherapeutic applications. The phosphorus-containing arm can be functionalised (e.g. with an ester moiety or some alkyl or aryl group) to afford bifunctional ligands that can be easily linked to a biologically active compound that determines the biodistribution of the final complex. The interaction of a paramagnetic Gd^{3+} complex with a macromolecule results in an increase in relaxivity due to the elongation of τ_R.

We have extended these studies to phosphorus-containing analogues of open-chain $DTPA^{5-}$ complexes. In this paper, we describe the synthesis and physicochemical characterisation of lanthanide complexes of three novel $DTPA^{5-}$ derivatives with a phosphorus acid pendant arm on the central nitrogen atom of the diethylenetriamine backbone, H_6L^1, H_5L^2 and H_5L^3 (see Scheme 1). Ligand H_6L^1 is the parent structure, while H_5L^2 is a ligand that, after appropriate substitution of the phenyl group, can be linked covalently to a polymer. Ligand H_5L^3 has a dibenzylamino moiety attached to the phosphorus function, a structural motif that has some similarity with that occurring in MS-325.[10] The Gd^{3+} complex of the latter ligand is known to be a very efficient blood-pool contrast agent due to its ability to bind noncovalently to human serum albumin (HSA).

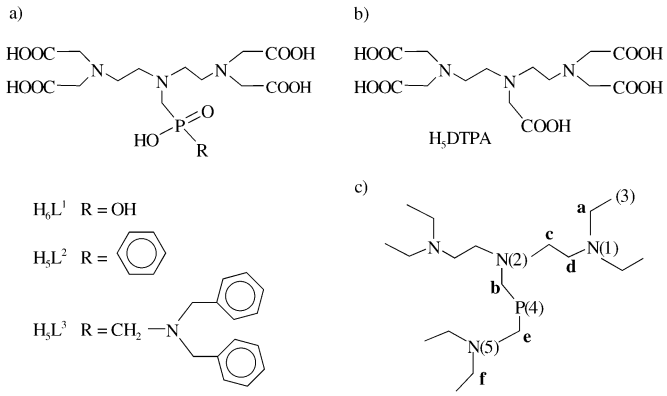

Scheme 1. Molecular structures of a) the ligands discussed and of b) H_5DTPA, c) atom-labelling scheme for NMR assignment.

Results and Discussion

Synthesis of the ligands: Attempts to build up the ligands from benzylamine (**2**) by treatment with tosylaziridine (**1**), followed by deprotection of the tosyl groups and alkylation with ethyl bromoacetate to give a H_5DTPA analogue with a *N*-benzyl-protected central amino group of the skeleton (**5**) were not successful due to the formation of a very stable lactam (**6**) after debenzylation (Scheme 2). This lactam was found to be extremely stable towards hydrolysis; it could be hydrolysed only under very harsh conditions (i.e., 20% NaOH, 90°C, overnight), affording the tetraacetic derivative (**7**). Therefore, it was decided first to attach the phosphorus-containing moiety to the diethylenetriamine backbone. This was achieved by a Mannich-type reaction between *N*,*N*″-bis(phthaloyl)diethylenetriamine (**8**), paraformaldehyde and the appropriate phosphorus derivative, followed by deprotection of phthaloyl moieties with hydrazine. Then, alkylation of intermediate (**10**) with ethyl bromoacetate and hydrolysis of the ester groups afforded the desired compounds H_6L^1, H_5L^2 and H_5L^3 in overall isolated yields of 50–80% (Scheme 3).

Determination of the ligand-protonation constants by using ^1H and ^{31}P NMR chemical-shift titrations: Since the thermodynamic stability of the Ln^{3+} complexes of aminocarboxylates is related to the summed protonation constants of the free ligand,[11–13] insight into the structural effects on these constants is desirable. Therefore, the protonation constants of all the ligands were determined by using the pH dependence of ^1H and ^{31}P NMR chemical shifts. The chemical shift curves (see Figure 1) display sharp changes at several ranges of pH values; they may be ascribed to the shift dependence on the changes of the protonation state of the ligand concerned.

Since the protonation equilibria are fast on the NMR timescale, the chemical shift of each signal can be given as a weighted average of the shifts of the various protonated species (see [Eq. (1)]).[14]

$$\delta_{obs} = \sum X_i \cdot \delta_i \qquad (1)$$

Here δ_{obs} is the observed chemical shift of a given signal, X_i is the molar fraction of species i and δ_i is its chemical shift. The observed ^1H and ^{31}P chemical shifts were fitted simultaneously according to Equation (1) by using the dissociation constants (pK_{ai}) and the values of δ_i as adjustable pa-

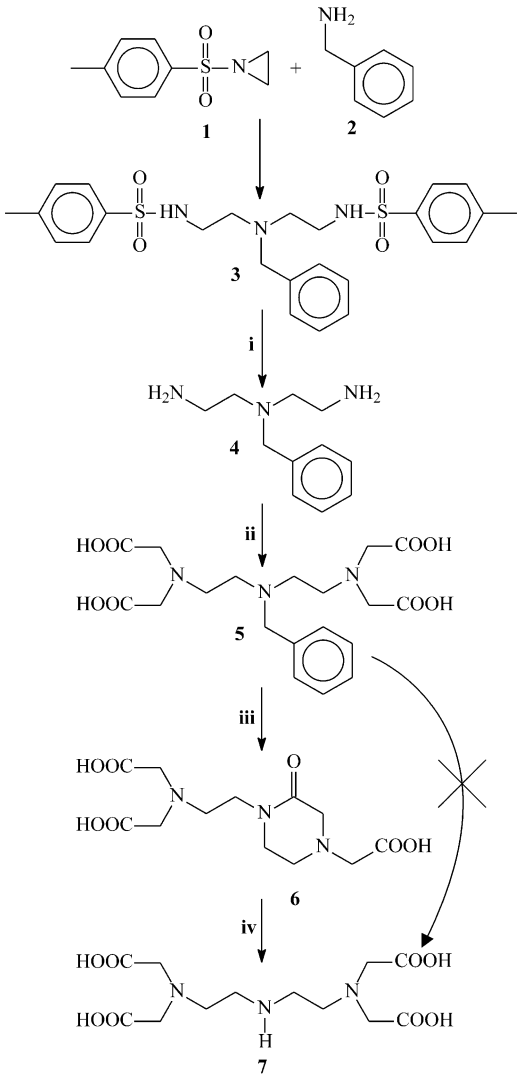

Scheme 2. Unsuccessful approach to ligand synthesis—formation of lactam (**6**), reagents: i) HBr; ii) $BrCH_2COOEt$, NaOH; iii) H_2, Pd/C; iv) NaOH.

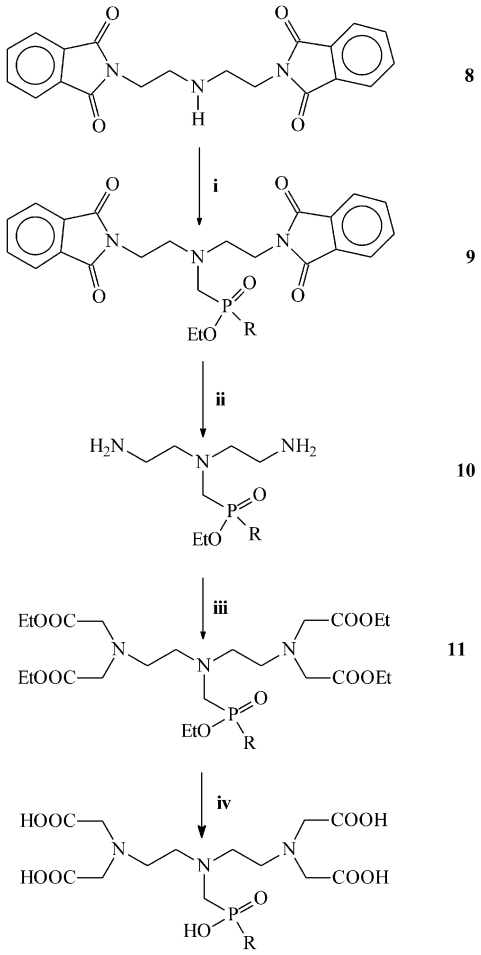

Scheme 3. Synthesis of H_6L^1 (R = OH), H_5L^2 (R = Ph) and H_5L^3 (R = $CH_2N(CH_2Ph)_2$); reagents: i) HP(O)(R)(OEt), CH_2O; ii) N_2H_4; iii) $BrCH_2COOEt$; iv) HCl or NaOH.

rameters. The fits of experimental data points are shown in Figure 1, and the resulting pK_a and δ_i values are compiled in Table 1 and the Supporting Information (Tables S1–S3), respectively. For comparison, pK_a values for H_5DTPA reported in the literature[15] are included in Table 1.

The ^{1}H NMR chemical shifts, $\Delta\delta_i^n$, calculated for each proton H_i at the various degrees of protonation of the ligands $(L^1)^{6-}$, $(L^2)^{5-}$ and $(L^3)^{5-}$ (see Tables S1–S3) were then used to evaluate the protonation fractions f_i (i = 1–5) at the nitrogen and oxygen basic sites of the ligands (Scheme 1c) for their successive protonated forms, with the empirical procedure of Sudmeier and Reilley.[14] This assumes that the chemical shifts of methylene protons in aminocarboxylates can be estimated by considering the effects of protonation of various basic sites to be additive and characteristic for the position of the given methylene group with respect to the protonation site, as expressed in Equation (2).

$$\Delta\delta_i^n = \sum C_N f_N + \sum C_{N'} f_N + \sum C_O f_O + \sum C_P f_P \qquad (2)$$

The protonation shifts of the methylene groups of the diethylenetriamine backbone reflect the protonation fractions of each of the terminal N(1) (f_1) and the central N(2) (f_2) nitrogen atoms of the ligands through the shielding constants C_N and $C_{N'}$ for the protonation of those amino groups, when they are at an α or β position, respectively, relative to those methylene groups (values of C_N = 0.75 ppm and $C_{N'}$ = 0.35 ppm have been listed).[14,15] The protonation fractions of the oxygen atoms at the terminal carboxylates O(3) (f_3) and at the central phosphonate group

Table 1. Dissociation constants (pK_a) of the ligands studied (0.1 M, 25 °C) and comparison with those of H_5DTPA.

	pK_{a1}	pK_{a2}	pK_{a3}	pK_{a4}	pK_{a5}	ΣpK_a
H_6L^1	10.747(5)	7.88(2)	6.92(7)	2.7(2)	2.17(6)	30.4
H_5L^2	9.60(5)	9.10(4)	2.63(19)	2.15(12)	0.72(14)	24.2
H_5L^3	10.1(1)	9.4(2)	7.13(2)	1.32(5)		28.0 (20.8)[a]
H_5DTPA[15]	10.2	8.6	4.2	2.9	1.8	27.7

[a] Values in parenthesis exclude the pK_a value associated with protonation of side-chain nitrogen atom.

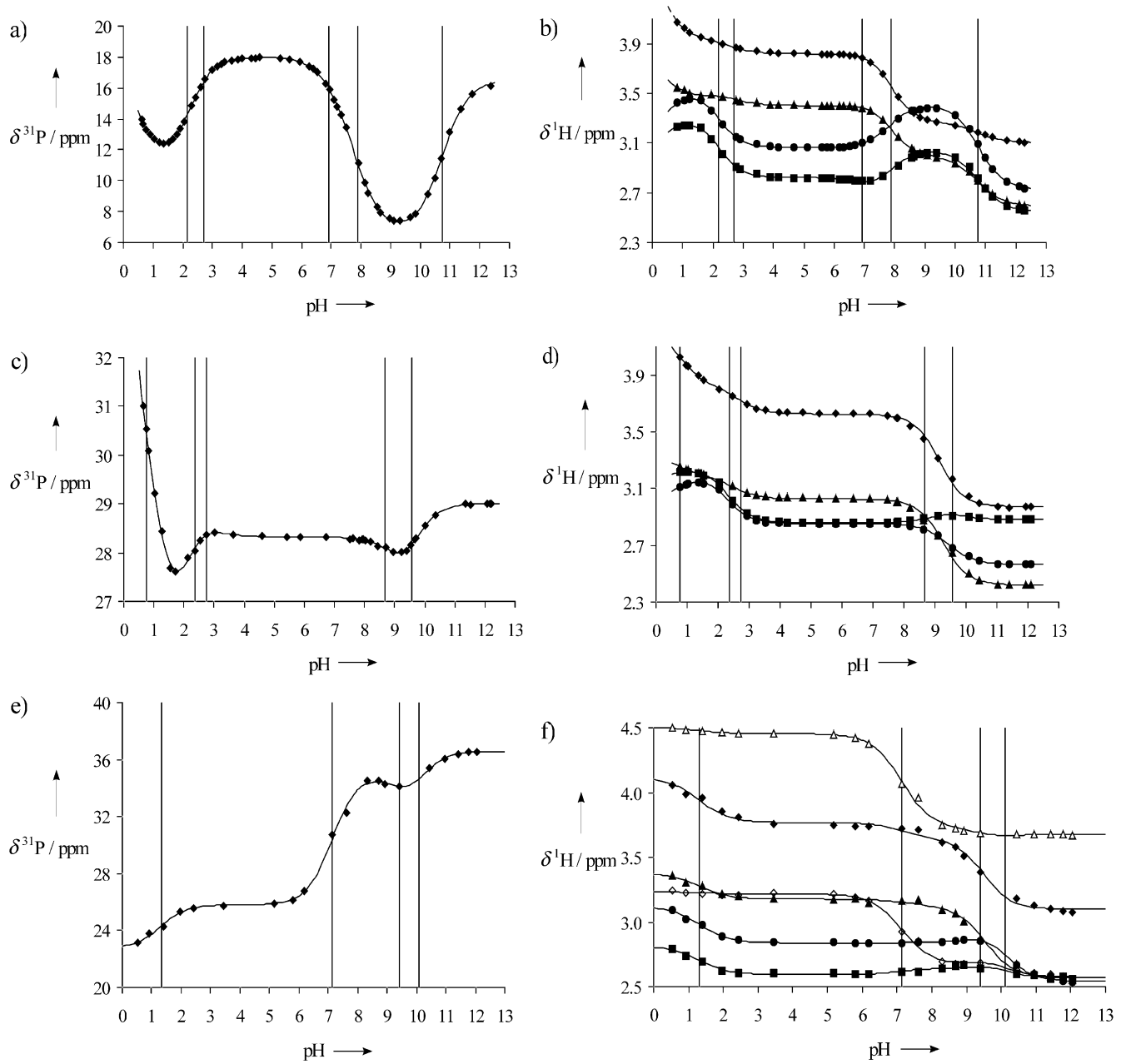

Figure 1. ^{1}H and ^{31}P NMR chemical-shift titration curves of 0.1 M solutions of H_6L^1 (a,b), H_5L^2 (c,d) and H_5L^3 (e,f) in H_2O/D_2O (9:1 *v/v*) at 25 °C and 7 T. Vertical lines mark the dissociation constants (for values, see Table 1). For labelling of hydrogen atoms see Scheme 1c: **a** (◆), **b** (■), **c** (●), **d** (▲), **e** (◇), **f** (△).

O(4) (f_4) were also calculated by using shielding constants C_O = 0.20 ppm for α-carboxylate protonation[15] and C_P = 0.20 ppm for α-phosphonate/phosphinate protonation.[16,17]

The results are given in Table 2 together with data for $DTPA^{5-}$ reported previously.[15] It can be seen that the first two protons bind exclusively to the backbone nitrogens in the three cases. The first protonation of the phosphonate ligand $(HL^1)^{5-}$ takes place mainly on the central nitrogen atom of the backbone (f_2), whereas in $HDTPA^{4-}$ and $(HL^3)^{4-}$, the preference for the central nitrogen is somewhat less, so that the central nitrogen atom is protonated to about the same extent as the sum of the two terminal ones. This is in agreement with the basicity of the nitrogen atom in aminomethylphosphonates, which is generally higher than that in aminomethylcarboxylates.[13] However, aminomethylphosphinates are less basic than the corresponding aminomethylcarboxylates; this explains why the central nitrogen atom (f_2) of the phenylphosphinic derivative $(L^2)^{5-}$ is only poorly protonated in the monoprotonated species $(HL^2)^{4-}$. In all cases, the protons of the $(H_2L)^{x-}$ species are located mainly on the outer nitrogen atoms (f_1), this can be rationalised by the electrostatic repulsion between the two incoming protons.

For $n>2$, the protonation also involves the basic atoms located at the pendant arms of the ligands. For the ligand $(L^1)^{6-}$, the f_i values show that the third protonation step mainly occurs at the phosphonate moiety; this is in agreement with its value of pK_{a3} (6.92) being close to the pK_a values commonly observed for phosphonates.[18] The next

Table 2. Percent protonation fractions of the different basic sites of the ligands $(L^1)^{6-}$, $(L^2)^{5-}$, $(L^3)^{5-}$ and $DTPA^{5-}$ in the protonated forms H_nL^{x-} at increasing values of n (for $DTPA^{5-}$, f_3 and f_4 correspond, respectively, to the terminal and central carboxylates. The errors in f_i values are ±10%).

H_nL^{x-}	f_1	f_2	f_3	f_4	f_5
$(H_nL^1)^{(n-6)-}$					
$n=1$	13	74	0	0	–
$n=2$	92	16	0	0	–
$n=3$	100	17	0	83	–
$n=4$	100	20	20	100	–
$n=5$	100	76	31	100	–
$(H_nL^2)^{(n-5)-}$					
$n=1$	46	8	0	0	–
$n=2$	100	0	0	0	–
$n=3$	100	8	23	0	–
$n=4$	100	48	38	0	–
$(H_nL^3)^{(n-5)-}$					
$n=1$	23	54	0	0	0
$n=2$	94	12	0	0	0
$n=3$	98	4	0	0	100
$n=4$	100	18	16	0	100
$(H_nDTPA)^{(n-5)-}$ [15]					
$n=1$	26	41	0	0	–
$n=2$	87	16	5	0	–
$n=3$	80	64	0	76	–

proton is mainly equally distributed over the four carboxylate oxygens, while the fifth shows a preference for the central nitrogen. In the cases of the phosphinate derivative ligands, $(L^2)^{5-}$ and $(L^3)^{5-}$, the central phosphinate oxygen is never protonated ($f_4 = 0$) under the conditions applied ($2 < pH < 13$), but the value of pK_{a3} of the second ligand (7.13) corresponds to protonation of the dibenzylamino moiety, as shown by the value $f_5 = 100\%$ (Table 2) and the shifts of the protons e and f next to the N(5) atom of its side chain (Figure 1f). Thus, for the $(L^2)^{5-}$ ligand, the third proton is about equally distributed over the four carboxylate oxygens, while the fourth binds preferentially to the central nitrogen. However, in the case of $(L^3)^{5-}$, the fourth proton is almost equally distributed over the four carboxylate oxygens and the central nitrogen atom.

This protonation scheme is qualitatively confirmed by the ^{31}P NMR titration curves (Figure 1a,c,e). Protonation of N(2) dramatically affects the charge density of the phosphorus atom of the phosphonate group, and to a lesser extent that of the phosphinate group. This can be ascribed to formation of a strong intramolecular hydrogen bond between $N(2)H^+$ and the phosphonate O^-, forming stable five-membered rings and resulting in a shift of the ^{31}P resonance to low frequency.[17,19] This can be seen in Figure 1, where low-frequency ^{31}P shifts are observed when N(2) and/or N(5) are protonated. Deprotonation of N(2) or protonation of the phosphonate/phosphinate group leads to high-frequency ^{31}P shifts, as both processes lead to the disappearance of the internal $NH^+\cdots O^-$ bonds.[17]

The sum of the pK_a values of the atoms of the ligand that are involved in binding to the Ln^{3+} ion of H_6L^1, H_5L^2 and H_5L^3 (for the last one, thus excluding the pK_a value associated with the protonation of the side-chain nitrogen atom, Table 1) is a good indication of the thermodynamic stability of the lanthanide complexes. Their values indicate that the complexes of the first two ligands will be comparable with those of the corresponding H_5DTPA complexes, whereas the protonation of the side-chain nitrogen of the third ligand is expected to lead to a somewhat reduced stability of the corresponding complexes.

The hydration numbers of the lanthanide complexes of H_6L^1, H_5L^2 and H_5L^3 as determined from the lanthanide-induced water ^{17}O NMR shifts: The ^{17}O NMR chemical shifts for water oxygen in 0.2 M solutions of complexes of all ligands with 14 different Ln^{3+} ions were measured at 40.7 MHz, 70 °C and pH 5–6. Under these conditions, the exchange between the Ln^{3+}-bound and bulk-water protons was rapid on the NMR timescale. Therefore, the observed chemical shifts with respect to free water (δ_{obs}, see Table S4 in the Supporting Information) are related to those of Ln^{3+}-bound water (δ_M) by Equation (3), in which q is the number of water molecules in the first coordination sphere of Ln^{3+} and ρ_w is the Ln^{3+}/water molar ratio in the sample. The bound shifts comprise diamagnetic (δ_d), contact (δ_c) and pseudocontact contributions (δ_p) [see Eq. (4)].[20]

$$\delta_{obs} = q \cdot \rho_w \cdot \delta_M \quad (3)$$

$$\delta_M = \delta_d + \delta_c + \delta_p \quad (4)$$

The contact contribution is the result of a through-bond transmission of unpaired-electron-spin density from the central ion to the ligand nucleus, and the pseudocontact contribution results from a dipolar interaction between the magnetic moment of the central ion and the nucleus in question. Both paramagnetic contributions, δ_c and δ_p, can be expressed as the product of lanthanide-dependent but ligand-independent constants ($\langle S_z \rangle$ and C_D, respectively) and terms characteristic for the nucleus under study (F and G, respectively) as given in Equation (5).

$$\Delta = \delta_{obs}/\rho_w = q(\langle S_z \rangle \cdot F + C_D \cdot G + \delta_d) \quad (5)$$

Values for $\langle S_z \rangle$ and C_D are tabulated in the literature.[21–25] For isostructural complexes, the ligand-dependent parameters F and G for the water ^{17}O nucleus are the same for all paramagnetic Ln^{3+} ions, and thus Equation (5) can be linearised in two different ways [Eqs. (6) and (7), in which $\Delta' = \Delta - q \cdot \delta_d$].[20] In other words, if the observed data afford linear plots according to Equations (6) and (7), it may be concluded that the complexes concerned are isostructural.

$$\frac{\Delta - q \cdot \delta_d}{C_D} = \frac{\Delta'}{C_D} = \frac{\langle S_z \rangle}{C_D} q \cdot F + q \cdot G \quad (6)$$

$$\frac{\Delta - q \cdot \delta_d}{\langle S_z \rangle} = \frac{\Delta'}{\langle S_z \rangle} = q \cdot F + \frac{C_D}{\langle S_z \rangle} q \cdot G \quad (7)$$

It has previously been shown that the value of parameter F is in the narrow range of 70 ± 11 for one coordinated oxygen-donor atom, independent of the nature of that atom and of the other ligands present in the Ln^{3+} complex.[20] Thus, the slopes of the plots of the experimental data according to Equation (6) are proportional to the number of

water molecules coordinated in the inner sphere of the Ln^{3+} ion.

The observed chemical shifts for the diamagnetic La^{3+} and Lu^{3+} complexes of the ligands under study were taken as $q{\cdot}\delta_d$. Plots of the values of Δ' for the Ln^{3+} complexes of the ligands studied according to Equation (6) were perfectly linear (see Figure 2a,c,e). The slopes of the lines and thus the values of $q{\cdot}F$ are -59, -65 and -70 for complexes of H_6L^1, H_5L^2 and H_5L^3, respectively. The values of $q{\cdot}F$ are close to that observed for H_5DTPA (-53),[26] in agreement with the presence of one water molecule in the inner coordination sphere of the Ln^{3+} ion for these complexes. This structural feature is the most common motif in the chemistry of Ln^{3+} complexes of H_5DTPA and related ligands.[1]

The plots according to Equation (7) (see Figure 3b,d,f) show a break between lighter (Ln = Ce→Eu) and heavier (Ln = Tb→Yb) Ln^{3+} ions, whereas the plots according to Equation (6) are linear. Such a break, observed exclusively in the former plots, can be ascribed to some small gradual changes of complex geometry[27] and/or to a change of crystal-field parameters along the lanthanide series.[28]

The pH dependence of the ^{17}O NMR shifts was studied in some detail for the Dy^{3+} complex of H_5L^2. A plot of the Δ values for this system as a function of the pH (see Supporting Information Figure S1) shows that, at pH close to 0, the value of Δ ($-21\,000$ ppm) is almost the same as that observed for the free Dy^{3+}–aqua ion ($-21\,685$ ppm), which has eight water molecules coordinated to the Dy^{3+} ion. Upon increase of the pH to 2.5, the value of Δ changes to about -3600 ppm; this reflects the substitution of 7 coordinated water molecules by the organic ligand, H_5L^2. Between pH 2.5 and 9.5, Δ is invariant, and no precipitation of hydroxides is observed; once again, this demonstrates the high stability of the complex formed.

Structure of the lanthanide complexes of H_6L^1 and H_5L^2 in solution as determined from ^{13}C and ^{31}P relaxation enhancements: The coordination number of Ln^{3+} ions in complexes of polyaminocarboxylates is, in general, nine. The ^{17}O NMR measurements described above show that one water molecule is bound in the first coordination sphere of the Ln^{3+} ion in the complexes of H_6L^1, H_5L^2 and H_5L^3. Therefore, it is most likely that these ligands are bound in an octadentate fashion, with binding occurring through the three nitrogen atoms of the backbone, four carboxylate oxygen atoms and one phosphonate/phosphinate oxygen atom. This is a binding mode similar to that of H_5DTPA itself. The NMR spectra of the Ln^{3+} complexes all displayed multiple resonances for the various types of nuclei. For example, the ^{13}C NMR spectrum of the diamagnetic complexes $[Y(L^1)(H_2O)]^{3-}$ and $[Y(L^2)(H_2O)]^{2-}$ at 25 °C showed two resonances in the carboxylate region (intensities 1:1) and some broad signals for the aliphatic ^{13}C nuclei. This indicates that several isomers of these complexes exist in solution and are in exchange with each other.

To support the coordination mode proposed, we evaluated the Nd^{3+}–C and Nd^{3+}–P distances from the ^{13}C and ^{31}P paramagnetic lanthanide-induced longitudinal-relaxation-rate enhancements. The Nd^{3+} ion was selected for this purpose, since it has the longest electron-spin-relaxation times among the light Ln^{3+} ions (Ln = Ce→Eu). The measurements were performed at 80 °C, at which temperature the spectra displayed relatively sharp lines ($\Delta\nu_{1/2} < 10$ Hz). In order to correct for diamagnetic contributions, the relaxation rates of the corresponding La^{3+} complexes were subtracted from the measured values for the Nd^{3+} complexes. Under the conditions employed, the ^{13}C NMR spectra of the Nd^{3+} complexes of H_6L^1 and H_5L^2 showed two carboxyl resonances, two resonances of carboxymethyl methylenes, two signals of the diethylenetriamine backbone and one doublet for the central methylene carbon, whereas the ^{31}P NMR spectra showed a single resonance. Since the outer-sphere contribution to longitudinal relaxation rates ($1/T_{1,OS}$) becomes significant only for remote

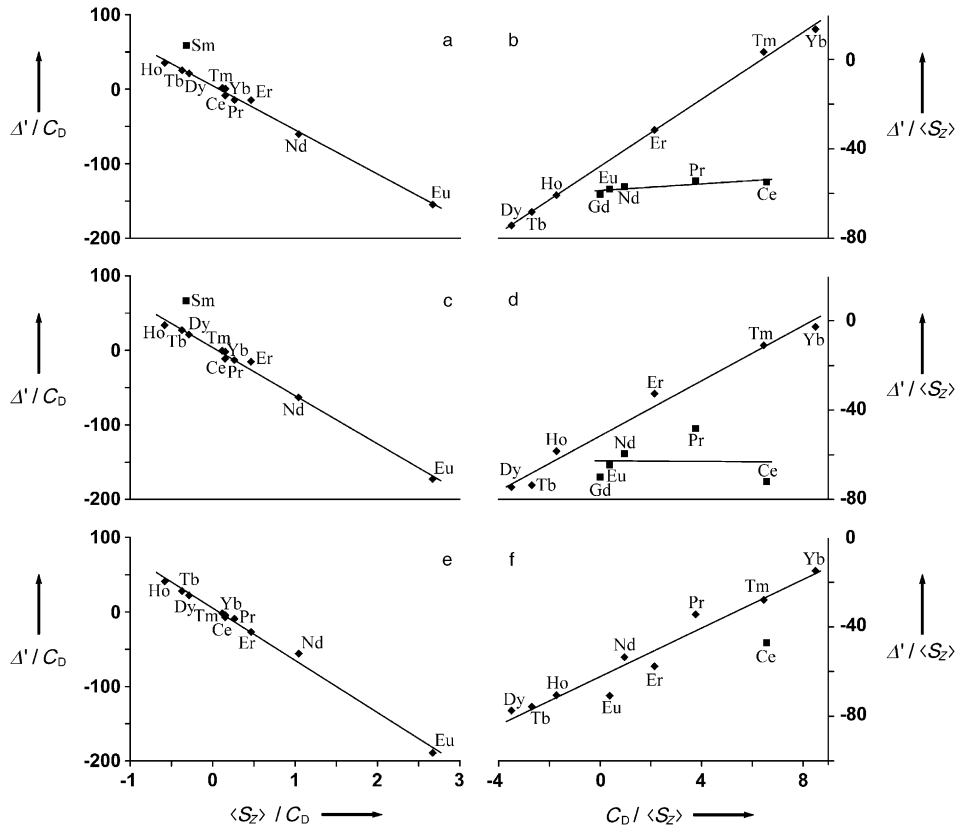

Figure 2. Linearisation of lanthanide-induced ^{17}O NMR shifts observed in D_2O solutions of the Ln^{3+} complexes of H_6L^1 (a,b), H_5L^2 (c,d) and H_5L^3 (e,f) according to Equations (6) and (7).

nuclei, this was neglected. From the electron-spin relaxation for Nd^{3+} ($T_{1e} \approx 10^{-13}$ s),[29] it can be estimated that the contact contribution to the paramagnetic relaxation is negligible. Therefore, two contributions are of importance: the dipolar relaxation and the Curie relaxation. These are represented by a combination of a simplified Solomon–Bloembergen equation with one for Curie relaxation, giving Equation (8):[20]

$$\frac{1}{T_1} = \left[\frac{4}{3}\left(\frac{\mu_0}{4\pi}\right)^2 \cdot \mu^2 \cdot \gamma_I^2 \cdot \beta^2 \cdot T_{1e} + \left\{\frac{6}{5}\left(\frac{\mu_0}{4\pi}\right)^2 \frac{\gamma_I^2 \cdot H_0^2 \cdot \mu^4 \cdot \beta^4}{(3k_B T)^2}\right\} \cdot \tau_R\right] \frac{1}{r^6} \quad (8)$$

Here $\mu_0/4\pi$ is the permeability of a vacuum, μ is the effective magnetic moment of Nd^{3+}, γ_I is the gyromagnetic ratio of the nucleus under study (^{13}C and ^{31}P), β is the Bohr magneton, T_{1e} is electronic spin relaxation time for Nd^{3+},[29] H_0 is the strength of the magnetic field, k_B is the Boltzmann constant, T is the temperature, τ_R is the rotational correlation time for the complex species and r is the distance of Nd^{3+} to the nuclei in the complex. This equation can be used to calculate the Nd^{3+}–C and Nd^{3+}–P distances r. For these calculations, values of τ_R at 80 °C of the corresponding Gd^{3+} complexes (23.1 ps for $[Nd(L^1)(H_2O)]^{3-}$ and 33.2 ps for $[Nd(L^2)(H_2O)]^{2-}$) were employed. These values were evaluated from variable-concentration ^2H NMR data performed on the deuterated La^{3+} complexes by using the activation energy for τ_R as obtained from the fitting of the ^{17}O and nuclear magnetic relaxation dispersion (NMRD) data (see below).Table 3 lists the experimental values of longitudinal relaxation rates observed for Nd^{3+} and La^{3+} complexes, together with the Nd^{3+}–C and Nd^{3+}–P distances calculated from them by using Equation (8). For comparison, results obtained for complexes of H_5DTPA and its bis(amide)derivatives reported previously[26,30,31] have been included in the Table. The similarity of these values confirms the proposed octadentate binding mode (similar to structures of well-known complexes of H_5DTPA) of the new ligands in their lanthanide complexes.

Interconversion between isomers of the Ln^{3+} complexes of the ligands under study: Upon binding of the ligands H_6L^1, H_5L^2 and H_5L^3 to a Ln^{3+} ion in an octadentate fashion through the diethylenetriamine nitrogen atoms, a phosphonate/phosphinate oxygen atom and four carboxylate oxygen atoms, the central nitrogen atom and the phosphorus atom become chiral. An inspection of crystal structures of Ln^{3+} complexes of DTPA derivatives has shown that the two ethylene moieties can adopt either a $\lambda\lambda$ or a $\delta\delta$ conformation.[32,33] Therefore, this is most likely to also be the case for the presently studied ligands. Then, four enantiomers (two diastereomeric pairs) are possible: $\lambda\lambda R$, $\lambda\lambda S$, $\delta\delta R$ and $\delta\delta S$, where R and S denote the chirality of the phosphorus atom. In a static situation, all ^{13}C nuclei in an isomer are chemically different. Therefore, for example four carboxylate resonances should be expected for each diastereomeric pair, leading to an expected total number of eight carboxylate resonances.

The variable-temperature behaviour of the ^{13}C NMR spectrum of the diamagnetic $[Y(L^2)(H_2O)]^{2-}$ complex was studied in some detail. At 0.5 °C, four carboxylate resonances of about equal intensity were observed. Upon increasing the temperature, these resonances broadened and coalesced to two resonances at about 9 °C, and sharpened again upon further temperature increase. Similar behaviour was observed for the other ^{13}C resonances; this indicates that a racemisation process becomes rapid on the NMR timescale. Racemisation of the central nitrogen atom can be achieved by a wagging motion of the diethylenetriamine moiety, which interconverts its $\lambda\lambda$ and $\delta\delta$ conformations. The phosphorus atom can racemise by decoordination of the phosphinate moiety followed by "inversion" of the phosphorus atom, that is, rotation around the CH_2–P bond and recoordination. Apparently, one of these two racemisation processes is already rapid on the NMR timescale at 0.5 °C, whereas the other becomes fast above 9 °C. From the coalescence temperature of the carboxylate resonances (9 °C), the free enthalpy of activation of the exchange process concerned (ΔG_{282}) can be estimated to be 56 ± 3 kJ mol^{-1}. The value is in the range of ΔG values generally found for the racemisa-

Table 3. Observed longitudinal relaxation rates in La^{3+} and Nd^{3+} complexes of ligands H_6L^1 and H_5L^2 and calculated nonbonding distances $r_{(Nd\text{-}P)}$ and $r_{(Nd\text{-}C)}$.

	longitudinal relaxation rates $1/T_1$ [s^{-1}]				distances from Nd^{3+} [Å]			
atom	La–H_6L^1	Nd–H_6L^1	La–H_5L^2	Nd–H_5L^2	H_6L^1	H_5L^2	H_5DTPA[a]	H_3DTPA-bis(amides)[b]
P	0.356	10.06	0.291	9.73	3.49	3.52		
*C*O	0.17[c]	6.02–6.25[c]	0.10[c]	6.29–8.93[c]	3.22–3.24[c]	3.03–3.22[c]	3.15–3.20	3.14–3.30
N-*C*H_2-CO	2.56[c]	7.04–7.46[c]	2.62[c]	7.52–7.69[c]	3.33–3.38[c]	3.33–3.35[c]	[d]	3.20–3.59
N-*C*H_2-P	3.00[e]	5.39[e]	1.72	8.71	3.76[e]	3.15	3.17[f]	3.14–3.30[f]
CH_2-N-*C*H_2-P	3.11	6.99	3.10	7.52	3.47	3.41	3.48[g]	3.04–3.48[g]
CH_2-N-*C*H_2-CO	2.82	7.09	3.11	8.40	3.41	3.30	3.21	3.04–3.48
P-*C*(arom)	–	–	0.11	1.96	–	3.94	–	–
C(arom-*o*)	–	–	0.72	1.29	–	4.79	–	–
C(arom-*m*)	–	–	0.70	0.89	–	5.75	–	–
C(arom-*p*)	–	–	1.28	1.41	–	6.13	–	–

[a] Taken from ref. [26]. [b] Taken from ref. [31]. [c] Two different signals of equal intensity are found in ^{13}C NMR spectra. [d] Not determined. [e] The signal has low intensity and overlaps others; this makes it unsuitable for the determination of relaxation rates. [f] Value corresponding to the signal of an acetate pendant moiety bound to the central nitrogen atom. [g] Value corresponding to the signal of a backbone carbon atom bound to the central nitrogen atom.

tion of the central nitrogen atom in Ln^{3+} complexes of H_5DTPA and its derivatives;[32,33] this suggests that the exchange process observed here can be assigned to such a racemisation. The racemisation at the phosphorus atom has a considerably lower barrier, as at 0 °C the exchange between the corresponding two enantiomeric forms is already rapid on the NMR timescale.

These results were confirmed by a variable-temperature and variable-pH study of the ^{1}H and ^{31}P NMR spectra of a 0.1 M aqueous solution of the diamagnetic $[La(L^3)(H_2O)]^{2-}$ complex. The ^{31}P and ^{1}H NMR signals of the complex were quite broad at 25 °C, but considerably sharpened at 60 °C. The proton resonances were assigned with the aid of a COSY spectrum at 60 °C, pH 6.4. A value of $pK_a = 6.58(4)$ was obtained from fitting the pH dependence of the ^{31}P and H_e and H_f resonances of the $[La(L^3)(H_2O)]^{2-}$ complex, with the protonation shift values indicating that the process occurs at the side-chain N(5) atom. At 60 °C, two resonances of about equal intensity were observed for each of the backbone ($H_{c,c'}$, $H_{d,d'}$) and acetate ($H_{a,a'}$, giving two AB patterns with $^2J_{HH}$ values of 16.6 Hz) protons of the complex, while only one sharp resonance was observed for each of the side-chain protons (singlet H_f, doublets H_e and H_b with $^2J_{PH}$ values of 9.8 and 8.0 Hz, respectively). This again indicates that at 60 °C the racemisation processes for the central nitrogen and the phosphorus atom are rapid on the NMR timescale.

Evaluation of rotational correlation times by ^{2}H NMR: The rotational correlation time, τ_R, is one of the parameters governing the relaxivity of a Gd^{3+} complex. Usually, a relatively large discrepancy exists between the τ_R^{298} values evaluated from the ^{1}H and ^{17}O NMR data. Therefore, we decided to determine the rotational correlation times independently using the deuterium longitudinal relaxation rates of the deuterated ligands $[D_8]H_6L^1$, $[D_8]H_5L^2$ and $[D_8]H_5L^3$ in their diamagnetic La^{3+} complexes.[34] In such a diamagnetic system, the deuterium relaxation depends only on quadrupolar interactions and is given by Equation (9):

$$R_1 = \frac{1}{T_1} = \frac{3}{8}\left(\frac{e^2qQ}{\hbar}\right)^2 \tau_R \qquad (9)$$

The quadrupolar coupling constant ($e^2qQ/\hbar$) has a value of $170\times 2\pi$ kHz for an sp^3-hybridised C–^{2}H bond. It has been demonstrated that τ_R values obtained in this way agree well with those obtained from ^{1}H NMRD measurements.[34] The $1/T_1$ values and, therefore, also the τ_R values for ^{2}H in samples of the La^{3+} complexes of the deuterated ligands were found to be dependent on the concentration of the complex for concentrations varying between 4 and 200 mM (Figure 3). Extrapolation of the curves in Figure 3 to the concentration used in the NMRD measurements (1 mM, see below) gave estimated values of 86, 110 and 121 ps for τ_R^{298} of the Gd^{3+} complexes of $[D_8]H_6L^1$, $[D_8]H_5L^2$ and $[D_8]H_5L^3$, respectively. The trend of these τ_R^{298} values agrees with the expected increase of the rotational correlation time upon increase of the molecular volume.

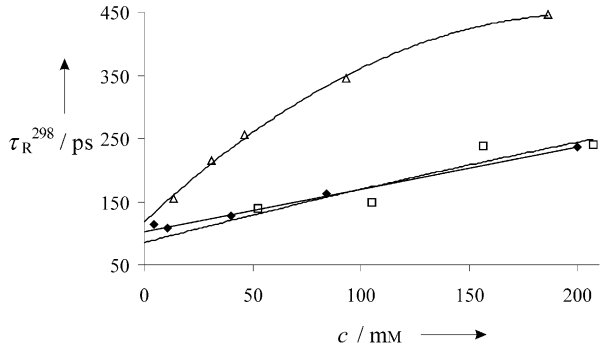

Figure 3. Rotational correlation times at 298 K (τ_R^{298}) obtained from solutions of $[La([D_8]L^1)(H_2O)]^{3-}$ (□), $[La([D_8]L^2)(H_2O)]^{2-}$ (◆) and $[La([D_8]L^3)(H_2O)]^{2-}$ (△) in H_2O at different concentrations.

Evaluation of the parameters governing the relaxivity from a variable-temperature ^{17}O NMR and ^{1}H NMRD study on the Gd^{3+} complexes: From a comparison of the observed longitudinal (T_1) and transversal (T_2) relaxation times and the frequencies (ω) of the ^{17}O NMR signal of water in the presence of Gd^{3+} complexes and the same parameters of the signal of pure water, the corresponding reduced parameters T_{1r}, T_{2r} and $\Delta\omega_r$ were calculated by using Equations (10) and (11):

$$1/T_{ir} = 1/P_m(1/T_i - 1/T_{iw}),\ \ i = 1,2 \qquad (10)$$

$$\Delta\omega_r = 1/P_m.(\omega - \omega_w) \qquad (11)$$

Here, the index "w" denotes the variable corresponding to pure water and P_m is the molar fraction of coordinated water. The calculated reduced variables are plotted in Figure 4a–f and listed in the Supporting Information (Tables S5–S7).

The magnetic-field dependence of the proton longitudinal relaxation was recorded as ^{1}H NMRD profiles at 5, 25 and 37 °C. The relaxation rates are, as usual, expressed in terms of relaxivity (r_1) in $s^{-1}mM^{-1}$ (see Figure 4g–i).

The ^{17}O NMR and ^{1}H NMRD data obtained were fitted with the sets of equations usually used to predict variable-temperature ^{17}O NMR data, with the Solomon–Bloembergen–Morgan equations (which describe the field dependency of the inner-sphere relaxivity, r_1) and with the Freed equation for the outer-sphere contribution of the relaxivity.[35] The set of equations used is given in the Supporting Information.

^{17}O NMR and ^{1}H NMRD data are influenced by a large number of parameters, many of which are common for these measurements. The fittings of these data were performed simultaneously; this has the advantage of putting constraints on these common parameters. Further constraints were achieved by fixing some of the parameters. It was assumed that the number of inner-sphere water molecules, q, is 1, the value that was obtained from the analyses of the Ln^{3+}-induced ^{17}O NMR shifts of bound water in the complexes under study (see above). The distance between Gd^{3+} and the oxygen atom of the coordinated water molecule, which is usually not dependent on the nature of the coordinated ligand,[36] was fixed at 2.5 Å. The distance between Gd^{3+}

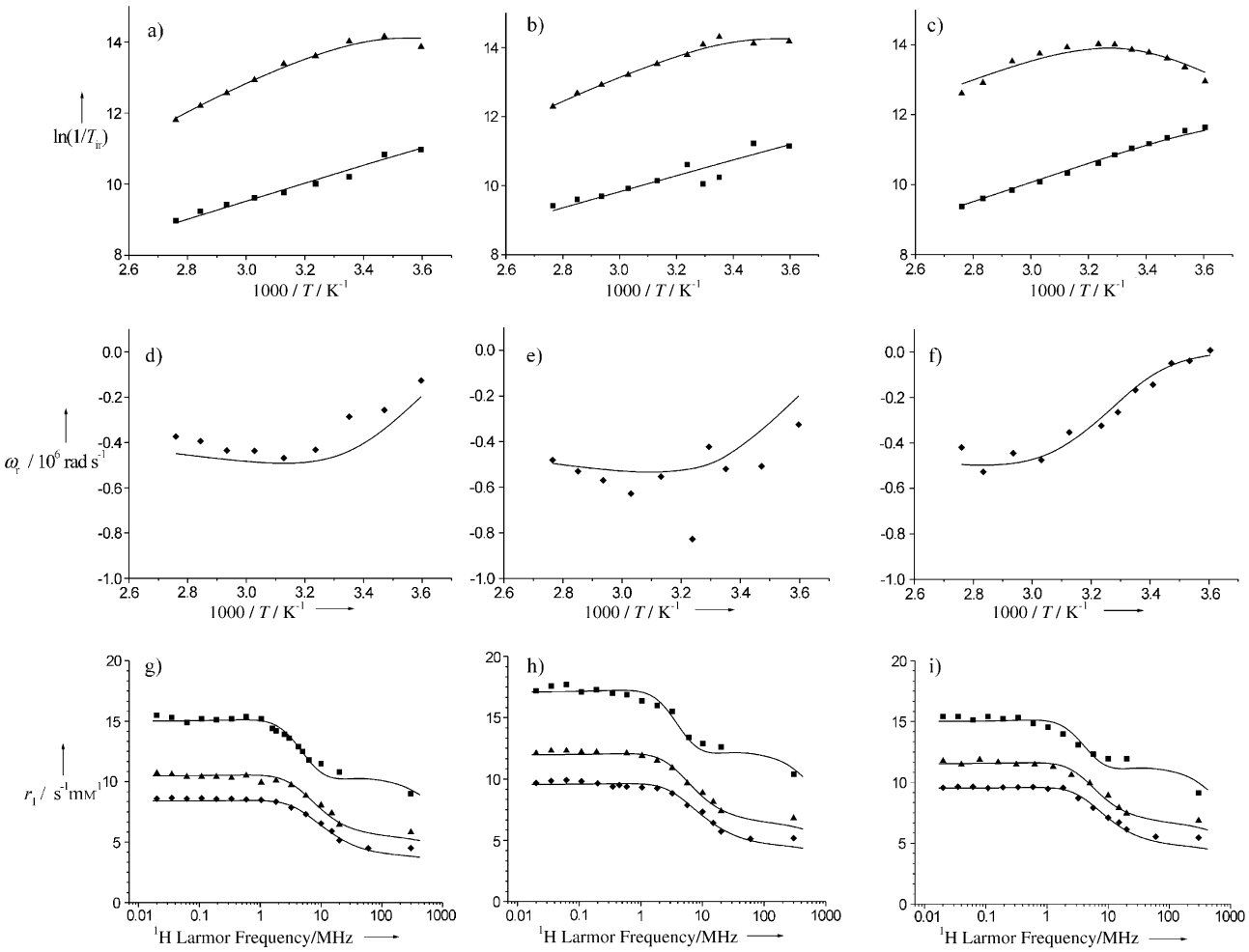

Figure 4. Simultaneously fitted data from ^{17}O NMR and ^{1}H NMRD measurements of $[Gd(L^1)(H_2O)]^{3-}$ (a,d,g), $[Gd(L^2)(H_2O)]^{2-}$ (b,e,h) and $[Gd(L^3)(H_2O)]^{2-}$ (c,f,i). First row (a,b,c): the temperature dependence of logarithms of the reduced relaxation rates (upper line (▲) corresponds to T_{2r}, lower line (■) corresponds to T_{1r}). Second row (d,e,f): the temperature dependence of the reduced frequency (◆). Third row (g,h,i): proton-relaxivity dependence on the magnetic field at 37 °C (◆), 25 °C (▲) and 5 °C (■).

and a water proton was fixed at 3.1 Å, whereas the distance of closest approach of a water molecule to Gd^{3+}, a^H, was fixed at 3.5 Å. The value of E_V, the activation energy of the correlation time τ_v, was fixed at 1 kJ mol^{-1}. Attempts to unfix this parameter led to negative values of the activation energy. The hyperfine coupling constants $A/\hbar$ were fixed at the values calculated from the F values obtained from the ^{17}O NMR studies described above and by using Equation (12), in which β is the Bohr magneton, k is the Boltzmann constant and γ_I is the ^{17}O magnetogyric ratio. Furthermore, the quadrupolar coupling constant of the bound water, $\chi(1+\eta^2)^{1/2}$, was taken equal to that determined recently for the complex $[Gd(dota)(H_2O)]^-$ of 5.2 MHz.[37]

$$F = \frac{\beta}{3kT\gamma_I}\frac{A}{\hbar}10^6 \qquad (12)$$

Fitting of the data with a single rotational correlation time resulted in bad fits, whereas separate fitting of the ^{17}O and NMRD data resulted in good fits, but with different τ_R values. This may be ascribed to the large difference in concentration at which the ^{17}O (200 mM) and the NMRD measurements (1 mM) were carried out (see above).[34] Furthermore, the ^{17}O and ^{1}H relaxation rates are modulated by rotation of the Gd–O and the Gd–H vectors, respectively. It may be expected that these rotations have different correlation times.[37] Therefore, two rotational correlation times were taken into consideration, τ_R^H and τ_R^O. The parameter τ_R^H was fixed at the values obtained from the ^{2}H NMR measurements (see above).

A comparison of the values of the fitted parameters of the complexes under study with those of $[Gd(dtpa)(H_2O)]^{2-}$ (see Table 4) reveals significant differences in the parameters related to the electronic relaxation (the square of the zero-field-splitting tensor, Δ^2, and the corresponding correlation time, τ_v and, particularly, in the diffusion coefficient, D_{GdH}, (see Table 4), which is unexpectedly low. D_{GdH} depends on the self-diffusion coefficients of the Gd^{3+} complex concerned, $D_{complex}$, and that of water, D_{water} [Eq. (13)].

$$D_{GdH} = D_{complex} + D_{water} \qquad (13)$$

Since D_{water} at 298 K is 2.23×10^{-9} m^2 s^{-1},[38] it should be expected that D_{GdH}^{298} is larger than this value. The relatively low

Table 4. Parameters for Gd^{3+} complexes as obtained from the simultaneous fitting of ^{17}O NMR and ^{1}H NMRD data by using a model including second-sphere water molecules and a model without second-sphere water molecules (see text), compared with literature values for $[Gd(dtpa)(H_2O)]^{2-}$ complex.

Parameter	$[Gd(L^1)(H_2O)]^{3-}$		$[Gd(L^2)(H_2O)]^{2-}$		$[Gd(L^3)(H_2O)]^{2-}$		$[Gd(dtpa)(H_2O)]^{2-}$ [a]
	no 2nd sphere	2nd sphere	no 2nd sphere	2nd sphere	no 2nd sphere	2nd sphere	no 2nd sphere
τ_M^{298} [ns]	62 ± 20	88 ± 26	74 ± 25	92 ± 29	543 ± 120	685 ± 297	303
$\Delta H^{\#}$ [kJ mol^{-1}]	38 ± 10	41 ± 8	36 ± 9	37 ± 8	29 ± 10	37 ± 9	51.6
$\tau_{R\ H}^{298}$ [ps]	86.4[b]	86.4[b]	109.5[b]	109.5[b]	121.0[b]	121.0[b]	58
E_R [kJ mol^{-1}]	14 ± 2	21 ± 3	15 ± 3	19 ± 3	20 ± 3	23 ± 3	17.3
$\tau_{R\ O}^{298}/\tau_{R\ H}^{298}$	2.3 ± 0.4	2.7 ± 0.4	2.5 ± 0.4	2.7 ± 0.4	3.5 ± 0.4	3.7 ± 0.4	–
τ_V^{298} [ps]	30 ± 3	22 ± 3	34 ± 3	26 ± 3	31 ± 3	25 ± 3	25
E_V [kJ mol^{-1}]	1[b]	1[b]	1[b]	1[b]	1[b]	1[b]	1.6
Δ^2 [10^{20} s^{-2}]	0.29 ± 0.03	0.45 ± 0.09	0.22 ± 0.02	0.32 ± 0.06	0.26 ± 0.03	0.36 ± 0.02	0.46
$\delta g_L^{\,2}$ [10^{-2}]	5 ± 2	6 ± 2	8 ± 2	8 ± 3	12 ± 2	11 ± 2	1.2
$A\,h^{-1}$ [10^6 rad s^{-1}]	−3.28[b]	−3.28[b]	−4.2	−3.61[b]	−3.69[b]	−3.69[b]	−3.8
D_{GdH}^{298} [10^{-10} m^2 s^{-1}]	14.3 ± 0.7	22.75[c]	13.2 ± 0.5	22.75[c]	12.4 ± 0.6	22.75[c]	20
$E_{D\,GdH}$ [kJ mol^{-1}]	28.7 ± 3	–	39.6 ± 3	–	25 ± 3	–	19.4
r_{GdO} [Å]	2.50[b]	2.50[b]	2.50[b]	2.50[b]	2.50[b]	2.50[b]	2.20
$\chi(1+\eta^2/3)^{1/2}$ [MHz]	5.2[b]	5.2[b]	5.2[b]	5.2[b]	5.2[b]	5.2[b]	14
q_{2s}	0	2.2 ± 0.4	0	2.0 ± 0.3	0	1.9 ± 0.3	–
r_{GdH2s} [Å]	–	3.5[b]	–	3.5[b]	–	3.5[b]	–
τ_{M2s}^{298} [ps]	–	35 ± 8	–	50 ± 9	–	60 ± 10	–
ΔH_{2s} [kJ mol^{-1}]	–	36 ± 11	–	48 ± 12	–	35 ± 10	
$\ln(1/T_{2e})$ exp[d]		23.65		23.47		23.25	
$\ln(1/T_{2e})$ calcd[e]		22.53		22.24		22.35	

[a] Taken from ref. [36]. [b] Parameters were fixed during the fitting. [c] Calculated with Equation (14), [d] Determined from EPR line widths; [e] Calculated by using fitted parameters.

values obtained for D_{GdH}^{298} indicate that the outer-sphere contribution to the total relaxivity is overestimated in the calculations. Most likely, this is due to an unaccounted contribution of water molecules in the second coordination sphere of Gd^{3+}, which may be bound to the ligand through hydrogen bonds to, for example, the negatively charged phosphinate/phosphonate group.[39] To account for such a contribution of second-sphere water molecules, we included a series of equations that are similar to those for the inner-sphere contribution (see Supporting Information). It should be noted, however, that it is very difficult to evaluate the second-sphere parameters because strong correlations exist among some of them. Moreover, the second-sphere water protons probably do not occupy a unique location but may exchange among various sites. We fixed the distance between the Gd^{3+} ion and the protons of the second-sphere water molecules, r_{2s}^{H}, at 3.5 Å in the fitting procedure. Furthermore, the values of D_{water}^{T} at various temperatures were calculated with the semiempirical relationship proposed by Hindman [Eq. (14)].[38] The size of the Gd^{3+} complexes of H_6L^1, H_5L^2 and H_5L^3 is much larger than that of water and, consequently, the self-diffusion constants of these complexes will be much smaller than that of water. In the present fittings $D_{complex}$ was, therefore, neglected.

$$-\ln D_{water}^{T} = \ln\left[3.11815\times10^{-4}\,e^{(5.06258\times10^3/T)} + 1.54792\times10^{2}\,e^{(1.62931\times10^3/T)}\right] \quad (14)$$

A good fit was obtained by assuming about two second-sphere water molecules ($q_{2s}\approx2$). The resulting optimised parameters are included in Table 4, and the results are also shown as curves in Figure 4g–i. Now, the optimised parameters obtained all compare well with those previously reported for $[Gd(dtpa)(H_2O)]^{2-}$.[36] The residence times of these second-sphere water molecules (τ_{M2s}^{298} = 35–60 ps) are of the same magnitude as those obtained for other systems.[39–41] Although the accuracy of the second-sphere parameters obtained may be low due to the many assumptions made, it is clear that at least two second-sphere water molecules, with a residence time that is sufficiently long to be detected, have to be included in the model to adequately explain the NMRD profile. Aime et al.[42] have reported that two second-sphere water molecules are present in $[Gd(pcp2a)(H_2O)_2]^{-}$, a complex of a pyridine containing macrocycle bearing one methylenephosphonic and two acetate arms. Apparently, phosphonate/phosphinate groups are capable of forming hydrogen bonds to two water molecules. Previously, it has been shown that second-sphere water molecules contribute to the relaxivity of several other phosphonate-bearing ligands including $[Gd(dotp)]^{5-}$ (H_8DOTP = 1,4,7,10-tetraazacyclododecane-1,4,7,10-tetrakis(methylphosphonic acid)).[42]

While the results of simultaneous fits of the present data gave a $\tau_{R\ O}^{289}/\tau_{R\ H}^{289}$ ratio of 2.7–3.0, the concentration dependence of τ_R as determined from ^2H NMR (see above) gave an estimate of this ratio of about 1.4 for equal concentrations. The latter value (1.4) is in agreement with that reported by Dunand et al. for the $[Gd(dota)(H_2O)]^{-}$ complex.[37] The differences between $\tau_{R\ H}^{289}$ and $\tau_{R\ O}^{289}$ may be ascribed to differences in the rotation rates of the Gd^{3+}–H and Gd^{3+}–O vectors.

The residence time of the Gd^{3+}-bound water molecule, τ_M, is an important parameter with regard to the efficiency of an MRI contrast agent. The theoretical curve of the relaxivity as a function of τ_M has a sharp maximum between 20 and 50 ns.[1,2,4] The values of τ_M^{298} for the $[Gd(L^1)(H_2O)]^{3-}$ and $[Gd(L^2)(H_2O)]^{2-}$ systems (88 and 92 ns, respectively)

are close to the optimum value. These τ_M values are lower than those of the current commercial contrast agents. For example, $[Gd(dtpa)(H_2O)]^{2-}$ and $[Gd(dota)(H_2O)]^{-}$ have τ_M^{298} values of 303 and 243 ns, respectively.[36] Consequently, it may be expected that very efficient MRI contrast agents can be obtained from $[Gd(L^2)(H_2O)]^{2-}$ by increasing its τ_R value through covalent or noncovalent binding to macromolecules. Unfortunately, the τ_M^{298} value of the $[Gd(L^3)(H_2O)]^{2-}$ complex is considerably higher (685 ns) and, thus, it may be expected that for this complex τ_M is limiting the relaxivity upon binding to a high-molecular-weight compound.

It has been shown that the water exchange in Gd^{3+}-polyaminocarboxylates with one Gd^{3+}-bound water generally takes place through a dissociative mechanism.[35] Then, steric strain at the water site may increase the energy of the initial state and, therefore, decrease the activation energy. The decrease in τ_M^{298} upon replacement of the central $-CH_2COO^-$ moiety in $[Gd(dtpa)(H_2O)]^{2-}$ by a $-CH_2PO_3^{2-}$ to form $[Gd(L^1)(H_2O)]^{3-}$ may be rationalised by an increase in steric strain around the Gd^{3+}-bound water molecule due to the relatively large size of the $-PO_3^{2-}$ function compared with the $-COO^-$ function. An inspection of molecular models shows that the phenyl group in $[Gd(L^2)(H_2O)]^{2-}$ is in the proximity of the Gd^{3+}-bound water. Most likely, $[Gd(L^3)(H_2O)]^{2-}$ has a preferred conformation with the phenyl groups at large distances from the water site. The nitrogen atom of the dibenzylamino moiety is protonated ($pK_a = 6.58$ for the corresponding La^{3+} complex, see above) and is in close proximity of the Gd^{3+}-bound water molecule. Possibly, the positive charge and the hydrogen bonding between these functions may slow down the water exchange rate and thus explain the rather long τ_M^{298} for this complex.

The temperature dependence of the NMRD profiles usually gives a good indication of the parameter limiting the proton relaxivity. If the relaxivity at high field (>10 MHz) increases with increasing temperature, it is limited by slow water exchange, whereas in the opposite case fast rotation is the limiting factor. From the temperature dependence of relaxivity at constant magnetic field (20 MHz, see Figure 5) it can be concluded that the total relaxivity decreases with increasing temperature, mainly because of a decrease of τ_R^{298}.

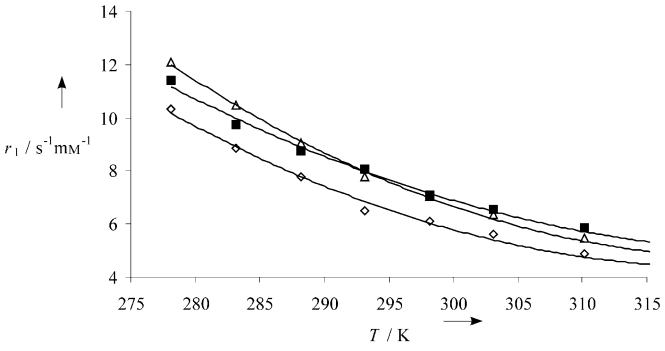

Figure 5. Relaxivity at 20 MHz as a function of temperature for $[Gd(L^1)(H_2O)]^{3-}$ (◇), $[Gd(L^2)(H_2O)]^{2-}$ (△) and $[Gd(L^3)(H_2O)]^{2-}$ (■). Experimental data were not fitted—the lines are only guides for the eye.

Evaluation of the electron-spin relaxation times T_{2e} of the Gd^{3+} complexes from EPR measurements: The X-band (0.34 T) EPR spectra of the Gd^{3+} complexes in aqueous solution at 298 K give approximately Lorentzian lines of $g \sim 2.0$. The transverse electronic relaxation rates ($1/T_{2e}$) were calculated from the experimental peak-to-peak line widths, ΔH_{pp}, by using Equation (15), in which the symbols have their usual meaning.[43]

$$1/T_{2e} = (g_L \mu_B \pi \sqrt{3h}) \Delta H_{pp} \quad (15)$$

The experimental values of ΔH_{pp} obtained at 298 K were 0.122 ± 0.05 mT ($[Gd(L^1)(H_2O)]^{3-}$), 0.103 ± 0.05 mT ($[Gd(L^2)(H_2O)]^{2-}$) and 0.182 ± 0.04 mT ($[Gd(L^3)(H_2O)]^{2-}$). The corresponding values of $\ln(1/T_{2e})_{exp}$ are compared in Table 4 with the $\ln(1/T_{2e})_{calcd}$ values calculated by using Equation (S9) (see Supporting Information), from the values of the parameters Δ^2 and τ_V^{298} obtained from the simultaneous fitting of the ^{17}O NMR and ^1H NMRD data. Although the relative experimental and calculated $1/T_{2e}$ values follow very similar trends in the three Gd^{3+} complexes, the experimental values are systematically larger by a factor of about three. This discrepancy has been noted before[36,44,45] and corrected by introducing both static and dynamic zero-field-splitting effects in the electronic relaxation mechanisms of Gd^{3+}.[46]

Interaction of $[Gd(L^3)(H_2O)]^{2-}$ with human serum albumin: To study the interaction between $[Gd(L^3)(H_2O)]^{2-}$ and HSA, a solution of the complex was added stepwise to a 4% solution of HSA in water. A nonlinear increase of the water-proton paramagnetic longitudinal relaxation rate was observed (see Figure 6) when plotted as a function of the concentration of the Gd^{3+} complex. The paramagnetic relaxation rate of a solution containing 0.81 mM of $[Gd(L^3)(H_2O)]^{2-}$ in 4% HSA is 3.9 times higher than that of 0.81 mM of $[Gd(L^3)(H_2O)]^{2-}$ in pure water; this indicates a strong interaction between the complex studied and HSA. This interaction is characterised by a stability constant (K_{AS}) of an adduct of HSA with the Gd^{3+} complex [Eq.

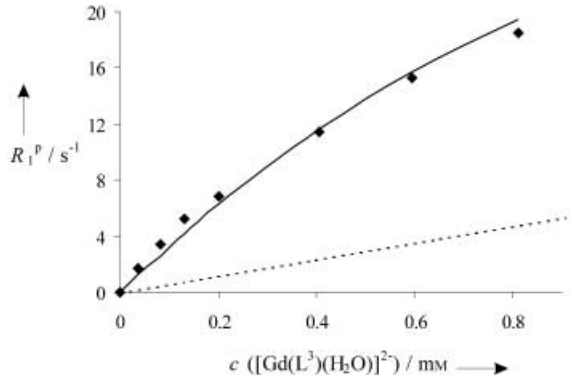

Figure 6. Proton longitudinal paramagnetic relaxation rates in solutions containing 4% HSA and increasing amounts of $[Gd(L^3)(H_2O)]^{2-}$ (◆) measured at 20 MHz and 310 K. The full line corresponds to the fitting of the data, and the dashed line represents R_1^p in an aqueous solution in the absence of albumin.

(16)].[47] The proton relaxivity data obtained in HSA, $R_1^{p\,obs}$, were fitted to Equation (17)]; here p^0 is the protein concentration, s^0 is the concentration of the paramagnetic complex, n is the number of independent interaction sites and r_1^c and r_1^f are the relaxivities of the $[Gd(L^3)(H_2O)]^{2-}$ complex when noncovalently bound to HSA and free, respectively. In this fitting procedure, the association constant, K_{AS}, and r_1^c were used as adjustable parameters.

$$n\,GdL + HSA \rightleftharpoons (GdL)_n{-}HSA \quad K_{AS} = \frac{[(GdL)_n{-}HSA]}{[GdL]^n\,[HSA]} \tag{16}$$

$$R_1^{p\,obs} = 1000 \times \left[(r_1^f \cdot s^0) + \frac{1}{2}(r_1^c{-}r_1^f)\left\{ (n \cdot p^0) + s^0 + K_{AS}^{-1} - \sqrt{((n \cdot p^0) + s^0 + K_{AS}^{-1})^2 - 4\,N \cdot s^0 \cdot p^0} \right\} \right] \tag{17}$$

A good fit between experimental and calculated values was obtained by using a model for one binding site ($n = 1$) with an association constant $K_{AS} = 4500 \pm 175\,M^{-1}$. The relaxivity of noncovalently bound complex (r_1^c) was calculated to be $43 \pm 0.4\,s^{-1}\,mM^{-1}$, while the value of the relaxivity of free complex (r_1^f) is $5.9 \pm 0.3\,s^{-1}\,mM^{-1}$ (see above). Thus, in a solution containing 0.81 mM of $[Gd(L^3)(H_2O)]^{2-}$ and 4% (0.6 mM) HSA, 48.4% of Gd^{3+} complex interacts with the protein.

Longitudinal relaxation rates of the solution containing 4% HSA and $[Gd(L^3)(H_2O)]^{2-}$ (0.81 mM) were measured at 310 K over the range of magnetic fields 4×10^{-4}–7.05 T. The corresponding NMRD profile (Figure 7a) shows the expected hump, characteristic for interactions with macromolecules, appearing in the high-frequency part ($\approx$20 MHz) of the recorded profile; this represents the combined contributions of the bound and free Gd^{3+} complex in the solution. The theoretical ^1H NMRD profile of the $[Gd(L^3)(H_2O)]^{2-}$-HSA adduct was then calculated from the known NMRD profile of free $[Gd(L^3)(H_2O)]^{2-}$ and the concentrations of free and bound complex obtained from the estimated stability constant of the adduct (see above) (Figure 7b). The relaxivities in the frequency region of importance for MRI (20–100 MHz) are similar to those of MS-325.[48] The NMRD curve of the $[Gd(L^3)(H_2O)]^{2-}$–HSA adduct could only be fitted with a model that assumed ten water molecules in the second sphere of the Gd^{3+} ion (see Figure 7b). A lower number of second-sphere water molecules always resulted in calculated relaxivities too low for the low-field part (<10 MHz) of the NMRD curve. The results of the fitting possibly reflect the presence of mobile HSA protons that are dipolarly relaxed by the proximity of the Gd^{3+} ion.[6] Alternatively, reduced mobility of solvent molecules in the second coordination sphere of Gd^{3+} upon noncovalent binding of $[Gd(L^3)(H_2O)]^{2-}$ to HSA can explain this result.

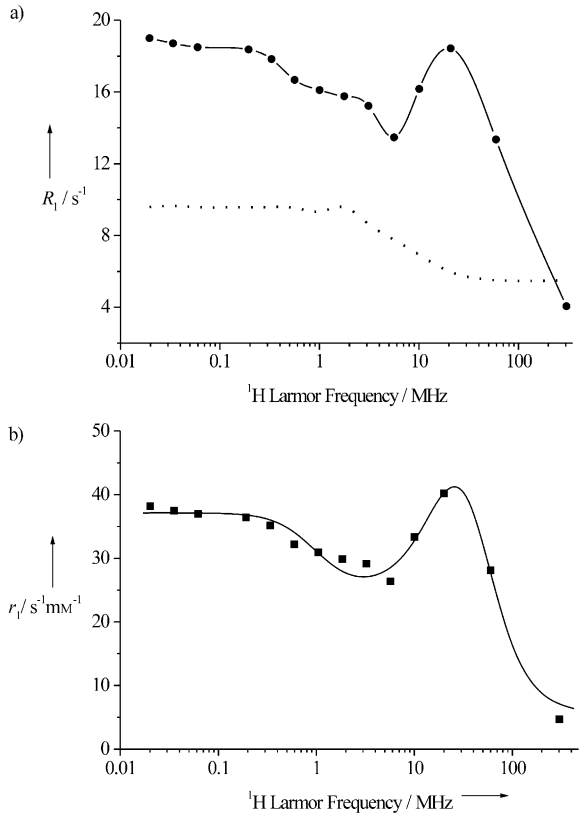

Figure 7. a) Proton-relaxation rate (R_1^p) of $[Gd(L^3)(H_2O)]^{2-}$ (0.81 mM) dissolved in 4% HSA (●). The dotted line corresponds to the proton-relaxation rate of $[Gd(L^3)(H_2O)]^{2-}$ in pure water at the same concentration. b) Calculated theoretical ^1H NMRD profile of the complex $[Gd(L^3)(H_2O)]^{2-}$ fully bound to human serum albumin at 310 K (■), ^1H NMRD profile of the complex simulated with the parameters obtained from simultaneous fit and optimal $\tau_R = 14$ ns.

Transmetallation: An important parameter determining the toxicity of Gd^{3+}-based contrast agents is the kinetic stability of the complexes. Transmetallation by endogenous metal ions may afford free Gd^{3+} ion, which is highly toxic. To get an impression of the kinetic stability of the phosphorus-containing complexes studied, we performed some transmetallation studies with Zn^{2+} according to a previously described protocol.[49]

Samples containing the Gd^{3+} complexes of H_6L^1, H_5L^2, H_5L^3 and a phosphate buffer containing $ZnCl_2$ were monitored by measuring the ^1H relaxivity at 20 MHz. Upon transmetallation with Zn^{2+}, the free Gd^{3+} formed immediately precipitated as the phosphate salt and, therefore, did not contribute to the total relaxivity any more. The resulting decrease in the proton-relaxation rate observed is a good estimate of the extent of transmetallation and, therefore, also for the kinetic stability of the Gd^{3+} complex. The results of the transmetallation experiments are displayed in Figure 8, while Table 5 shows the percentage of Gd^{3+} complexes left in the solution after 3 d. Thus, the kinetic stability decreases in the following order: $[Gd(dtpa)(H_2O)]^{2-} \gg [Gd(L^1)(H_2O)]^{3-} \geq [Gd(L^3)(H_2O)]^{2-} \geq [Gd(dtpa\text{-}bma)(H_2O)] > [Gd(L^2)(H_2O)]^{2-}$. Therefore, all complexes studied are less stable towards Zn^{2+} transmetallation than $[Gd(dtpa)(H_2O)]^{2-}$, but $[Gd(L^1)(H_2O)]^{3-}$ and $[Gd(L^3)(H_2O)]^{2-}$ are slightly more kinetically stable than $[Gd(dtpa\text{-}bma)(H_2O)]$.

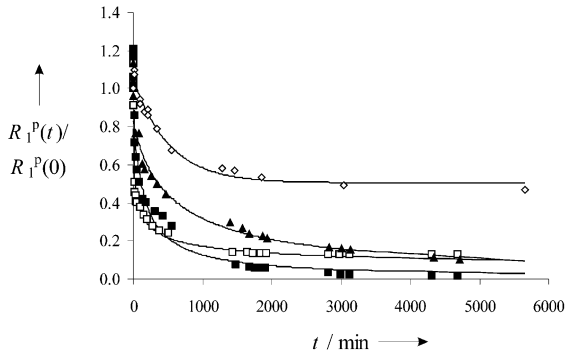

Figure 8. Evolution of the relative water proton paramagnetic longitudinal relaxation rate $R_1^p(t)/R_1^p(0)$ vs. time for $[Gd(dtpa)(H_2O)]^{2-}$ (◇), $[Gd(L^1)(H_2O)]^{3-}$ (□), $[Gd(L^2)(H_2O)]^{2-}$ (■) and $[Gd(L^3)(H_2O)]^{2-}$ (▲). The lines are only guides for the eye. The solution initially contained Gd^{3+} complex (2.5 mM), $ZnCl_2$ (2.5 mM) and phosphate ($H_2PO_4^-$, HPO_4^{2-}, PO_4^{3-}, 67 mM).

Table 5. Percentage of remaining Gd^{3+} complexes after 3 d of transmetallation with Zn^{2+}.

Complexes	$R_1^p{}_{(t=3d)}/R_1^p{}_{(t=0)}$ [%]
$[Gd(L^1)(H_2O)]^{3-}$	13
$[Gd(L^2)(H_2O)]^{2-}$	1.9
$[Gd(L^3)(H_2O)]^{2-}$	11
$[Gd(dtpa)(H_2O)]^{2-}$	49
$[Gd(dtpa\text{-}bma)(H_2O)]$	9

Conclusion

A useful synthetic approach for a new class of H_5DTPA-based ligands in which the central pendant arm has a –P(OH)(O)R moiety is reported. Their Ln^{3+} complexes show structural features analogous to the H_5DTPA complexes, including the presence of one water molecule coordinated in the first coordination sphere of the metal ion. The phosphonate (H_6L^1) and the phenylphosphinate derivatives (H_5L^2) have τ_M^{298} values that are close to optimal (88 and 92 ns, respectively). Therefore, these complexes are very suitable for attachment to polymers, which should result in compounds with very high relaxivity. The relaxivity will be less limited by water exchange than in most conjugates of chelates of the H_5DTPA or H_4DOTA type. Furthermore, an additional increase in the relaxivity is obtained by virtue of the presence of two water molecules in the second coordination sphere and which are probably bound to the phosphonate/phosphinate moiety through hydrogen bonds. The $[Gd(L^3)(H_2O)]^{2-}$ complex has a less favourable water-exchange rate (τ_M^{298} = 685 ns), but it has a high affinity to HSA and a relaxivity that is comparable with that of the well-known blood pool contrast agent MS-325.

Experimental Section

Materials and methods: Commercially available benzylamine (**2**), diethylenetriamine, phthalanhydride, ethyl chloroformate, ethyl bromoacetate, diethylphosphite and phenylphosphinic acid had synthetic purity and were used as received. The 10% Pd/C catalyst for the hydrogenation reactions was obtained from Acros. Bis(phthaloyl)diethylenetriamine (**8**),[50] ditosylethanolamine,[51] *N*-tosylaziridine (**1**),[52] and ethyl phenylphosphinate[53] were prepared by published methods. Paraformaldehyde was obtained by filtration of aged aqueous formaldehyde solutions and was dried in a desiccator over concentrated sulfuric acid.

^1H (300 MHz), ^2H (46.1 MHz), ^{13}C (75.5 MHz), ^{17}O (40.7 MHz) and ^{31}P NMR spectra (121.5 MHz) were recorded on a Varian INOVA-300 spectrometer with 5 mm sample tubes. Unless stated otherwise, NMR experiments were performed at 25 °C. Chemical shifts are reported as δ values and are given in ppm. For measurements in D_2O, *tert*-butyl alcohol was used as an internal standard with the methyl signal calibrated at 1.2 ppm (^1H) or 31.2 ppm (^{13}C). Deuterium oxide (100%) was used as an external chemical-shift reference for ^{17}O resonances. The ^{31}P chemical shifts were measured with respect to 1% H_3PO_4 in D_2O as an external standard (substitution method). The pHs of the samples were measured at ambient temperature by using a Corning 125 pH meter with a calibrated microcombination probe from Aldrich. The pH values of the solutions were adjusted by using dilute solutions of NaOH and HCl. The variable-temperature ^{17}O measurements were performed at a magnetic field of 7.05 T on a Varian INOVA-300 spectrometer equipped with a 5 mm probe. Thin-layer chromatography was performed on silica-coated aluminium sheets (Silufol, Kavalier, Czech Republic).

Mass spectra were obtained with a VG AUTOSPEC 6F mass spectrometer (VG Analytical, Manchester, UK) or on a Bruker ESQUIRE 3000 with ion-trap detection in positive or negative modes.

Preparation of *N′*-benzyldiethylenetriamine (4): *N*-tosylaziridine (**1**) (32.0 g, 162 mmol) was dissolved in ethanol (150 mL). Benzylamine (**2**) (8.00 g, 75 mmol) was added, and the solution was heated under reflux for 3 days. Then, the mixture was cooled and concentrated aqueous ammonia (5 mL) was added to quench the excess of tosylaziridine. The mixture obtained was heated under reflux for 15 min. Solvents were removed, and the residual brown oil was dissolved in a mixture of concentrated HBr/AcOH (300 mL, 1:1, *v*/*v*). The solution was heated under reflux for 24 h. After cooling, the reaction mixture was evaporated to dryness leaving a brown oil, which solidified upon cooling. This solid was dissolved in NaOH (100 mL, 15%), and the solution obtained was extracted with chloroform (7×50 mL). The organic phases were combined and evaporated to dryness to leave the mixture of monotosylated intermediate and the required product as a yellow oil. These compounds were separated by chromatography on silica by using gradient elution with increasing concentration of concentrated ammonia in ethanol from a ratio of 1:25 (mixture A) to 1:5 (mixture B), detection by ninhydrine (purple spots). Note: extension of the reaction period to 36–48 h reduces the yield of the final product due to decomposition.

Yield: 8.25 g (57%), R_f (mixt. A) = 0.1, R_f (mixt. B) = 0.3; ^1H NMR ($CDCl_3$): δ = 2.05 (br, 4H; NH_2), 2.52, 2.75 (2m, 4H; NCH_2CH_2N), 3.58 (s, 2H; NCH_2Ph), 7.31 (m, 5H; *Ph*); ^{13}C NMR ($CDCl_3$): δ = 34.58 (2C), 57.05 (2C, NCH_2CH_2N), 59.14 (1C, $PhCH_2N$), 127.02 (1C), 128.30 (2C), 128.86 (2C) and 139.49 (1C, all *Ph*); ESI-MS: positive *m*/*z*: 194.0 $[M+H]^+$.

***N*-Tosyl-*N′*-benzyldiethylenetriamine**: Yield: 4.55 g (18%); R_f (mixt. A) = 0.8, R_f (mixt. B) = 0.9; ^1H NMR ($CDCl_3$): δ = 2.40 (s, 3H; CH_3), 2.49 (m, 2H), 2.58 (m, 2H), 2.76 (m, 2H) and 2.95 (m, 2H; all NCH_2CH_2N), 3.05 (br, 1H; NH), 3.52 (s, 2H; NCH_2Ph), 7.20 (m, 2H; *Ts*), 7.27 (m, 5H; *Ph*), 7.73 (m, 2H; *Ts*); ^{13}C NMR ($CDCl_3$): δ = 22.12 (1C, CH_3), 39.73, 42.11, 53.14, 55.99 (4×1C, NCH_2CH_2N), 59.83 (1C, NCH_2Ph), 127.67 (2C), 127.82 (1C), 129.01 (2C), 129.45 (2C), 130.20 (2C), 137.82 (1C), 139.51 (1C), 143.58 (1C); ESI-MS: positive *m*/*z*: 348.3 $[M+H]^+$.

Preparation of *N′*-benzyldiethylenetriamine-*N*,*N*,*N″*,*N″*-tetraacetic acid (5): *N′*-benzyldiethylenetriamine (**4**) (1.00 g, 5.2 mmol) was dissolved in water (5 mL) and then 1 mL of a solution of NaOH (2.5 g, 62.5 mmol, dissolved in 10 mL of water) was added. The mixture was heated to 90 °C. Ethyl bromoacetate (4.34 g, 26 mmol) and the remaining NaOH solution were added in 6 portions during 1.5 h. The solution was then heated under reflux for 24 h to hydrolyse the ester groups. After cooling, the mixture was poured onto a column containing a strong cation exchange resin (150 mL, Dowex 50) in the H^+ form. The column was washed with water and the product was eluted with diluted aqueous ammonia (1:3). The eluate was evaporated to dryness to leave the crude

product as a yellow oil. This product was purified by chromatography on a strong anion exchanger (Dowex 1) in the acetate form. After washing with 10% AcOH, the product was eluted with 5% HCl. The product was precipitated as a nonstoichiometric hydrochloride (2.5–3 equiv HCl per ligand molecule) upon trituration in acetone. Yield: 2.10 g (~75%); ^{1}H NMR (D_2O, pD 2.5): δ = 2.95 and 3.17 (br, 8H; NCH_2CH_2N), 3.57 (s, 8H; NCH_2CO), 3.62 (s, 2H; NCH_2Ph), 7.36 (m, 5H; *Ph*); ^{13}C NMR (D_2O, pD 2.5): δ = 48.60 (2C, NCH_2CH_2N), 53.70 (2C, NCH_2CH_2N), 58.26 (4C, NCH_2CO), 59.30 (1C, NCH_2Ph), 129.54 (1C, *Ph*), 130.42 (2C, *Ph*), 131.07 (2C, *Ph*), 138.50 (1C, *Ph*), 171.53 (4C, *C*O).

Preparation of the lactam of diethylenetriamine-*N,N,N′,N″*-tetraacetic acid (6): *N*-benzylated tetraacetate (**5**) (1.00 g of the hydrochloride) was dissolved in water (10 mL). Acetic acid (5 mL) was added, followed by 10% Pd/C catalyst (0.10 g). The mixture was stirred at room temperature under a hydrogen atmosphere for 48 h. Then the catalyst was removed by filtration, and all solvents were evaporated in vacuo. The product was purified by chromatography on Dowex 1 in the acetate form (75 mL). Some unidentified impurities were eluted with acetic acid (1–5% in water) and, subsequently, the required product was eluted with 10% AcOH. Evaporation of solvents afforded the product as yellowish oil (0.56 g, 95%). ^{1}H NMR (D_2O, pD 3.5): δ = 2.5–2.7 (br, 8H; NCH_2CH_2N), 3.03 (2H), 3.13 (s, 2H; CH_2CO), 3.18 (s, 4H; CH_2CO); ^{13}C NMR (D_2O, pD 3.5): δ = 44.40, 44.90, 50.41, 54.22 (4×1C, NCH_2CH_2N), 56.19 (1C, NCH_2CO), 56.36 (2C, NCH_2CO), 57.33 (1C, NCH_2CO), 166.56 (1C, *C*ON), 168.63 (1C) and 169.51 (2C, *C*OO).

Preparation of diethylenetriamine-*N′*-methylenephosphonic-*N,N,N″,N″*-tetraacetic acid (H_6L^1): Bis(phthaloyl)diethylenetriamine (**8**) (10.00 g, 27.5 mmol) and diethylphosphite (11.4 g, 82.5 mmol) were dissolved in a mixture of toluene (100 mL) and dry ethanol (30 mL), then the mixture was heated under reflux with a Dean–Stark trap. Over a period of 6 h, paraformaldehyde (2.48 g, 82.5 mmol) was added in portions. The reaction mixture was heated under reflux for another 12 h. After cooling, the mixture was filtered and the solvent was evaporated under vacuum.

^{13}C NMR of intermediate (**9**) ($CDCl_3$): δ = 16.08 (2C, *C*H$_3$), 35.00 (2C, NCH$_2$*C*H$_2$NPht), 48.24 (d, $^1J_{CP}$=150 Hz, 1C, N*C*H$_2$P), 52.47 (2C, N*C*H$_2$CH$_2$NPht), 61.45 (2C, PO*C*H$_2$), 122.66, 131.79 and 133.61 (all Ph*t*), 167.64 (4C, *C*O). Signals due to the excess of diethylphosphite overlapped the ethoxy resonances of the product in spectra of the crude mixture. Furthermore, an additional signal of diethyl hydroxymethylphosphonate (doublet of N*C*H$_2$P centred at 57.5 ppm) was observed.

The material obtained was dissolved in dry ethanol (60 mL). Hydrazine hydrate (3.44 g, 68 mmol) was added, and the mixture was heated under reflux for 6 h. Precipitation of phthalhydrazide began after ~10 min of reflux. The mixture was cooled, and phthalhydrazide was filtered off. The ethanol was evaporated, and water was removed by co-distillation with dry ethanol.

The intermediate obtained (**10**) was dissolved in DMF (70 mL), and then $BrCH_2CO_2Et$ (36.7 g, 220 mmol, 8 equiv) and K_2CO_3 (30.4 g, 220 mmol) were added. The mixture was stirred at room temperature for 18 h. The solids were filtered off, after which the reaction mixture was diluted with a saturated aqueous solution of $NaHCO_3$ (70 mL). Subsequently, the product was extracted into toluene (200 mL). The organic layer was washed with a saturated solution of $NaHCO_3$ (70 mL) and of brine (70 mL). The toluene phase was dried over Na_2SO_4, filtered and then evaporated to dryness. NMR of intermediate (**11**): ^{1}H NMR ($CDCl_3$): δ = 1.16 (m, 18H; CH_3), 2.80 (m, 8H; backbone CH_2), 3.04 (d, $^2J_{CP}$=10 Hz, 2H; NCH_2P), 3.51 (s, 8H; CH_2CO$_2$), 4.15 (m, 12H; OCH_2); ^{31}P NMR ($CDCl_3$): δ = 26.00. ESI-MS: positive *m*/*z*: 598.4 $[M+H]^+$.

The crude ethyl ester (**11**) obtained above was dissolved in diluted HCl (250 mL, 1:1), and the mixture was heated under reflux for 18 h. During this time, some precipitate (probably remains of phthalic acid) was formed. The mixture was filtered and then evaporated to dryness.

The residue was dissolved in water and poured onto a column of cation exchange resin (Dowex 50, 170 mL, H^+ form). Nonbasic compounds were removed by elution with water. The crude product was eluted using a diluted ammonia (1:3) solution. The yellow fraction was evaporated to dryness, dissolved in water and then purified by chromatography on an anion exchange column (Dowex 1, 250 mL, acetate form). After being washed with water, some yellow impurities were removed by elution with 10% acetic acid. The product was collected in diluted HCl (3%) fractions. The fractions containing the product were evaporated to dryness leaving a glassy solid, which was dissolved in small amount of water and crystallised by standing for several days. The white solid obtained was filtered, washed with acetone and air-dried. Yield: 10.15 g (76%); m.p. 133–135°C (dec.); ^{1}H NMR (D_2O, pD 0.7): δ = 3.01 (2H; NCH_2P), 3.22 (4H; NCH_2CH_2N) 3.39 (4H; NCH_2CH_2N), 3.96 (8H; NCH_2CO); ^{13}C NMR (D_2O, pD 0.7): δ = 49.64 (d, $^1J_{CP}$=147 Hz, 1C, NCH_2P), 50.89 (2C, PCH$_2$NCH_2), 51.86 (2C, PCH$_2$NCH$_2$CH_2N), 55.30 (4C, NCH_2CO), 169.56 (4C, *C*O); ^{31}P NMR (D_2O, pD 0.7): δ = 15.75; elemental analysis calcd (%) for H_6L^1·HCl·H_2O ($C_{13}H_{27}ClN_3O_{12}P$, M = 483.79): C 32.27, H 5.63, Cl 7.33, N 8.69; found: C 31.90, H 5.49, Cl 7.33, N 8.45; ESI-MS: positive *m*/*z*: 430.3 $[M+H]^+$; negative *m*/*z*: 428.3 $[M-H]^-$.

Preparation of diethylenetriamine-*N′*-methylene(phenyl)phosphinic-*N,N,N″,N″*-tetraacetic acid (H_5L^2): Freshly prepared ethyl phenylphosphinate[53] (13.80 g, 81.1 mmol, 2.9 equiv) was transferred into a 250 mL flask and dissolved in a mixture of toluene (150 mL) and dry ethanol (30 mL). Bis(phthaloyl)diethylenetriamine (**8**) (10.00 g, 27.5 mmol) was added, and then the mixture was heated under reflux with a Dean–Stark trap. During the next 6 h, paraformaldehyde (2.48 g, 82.5 mmol, 3 equiv) was added in portions. The solvent in the trap was removed, and then the mixture was heated for another 14 h at 100°C. The mixture was cooled and filtered. Ethyl hydroxymethyl(phenyl)phosphinate formed as a by-product (δ = 40.1 ppm in ^{31}P NMR spectra) and some starting ethyl phenylphosphinate were extracted with water (10×50 mL), the organic layer was dried over Na_2SO_4 and then evaporated to dryness leaving a yellow oil. ^{31}P NMR spectra indicated that the product (**9**) was contaminated with a small amount of starting ethyl phenylphosphinate. ^{13}C NMR ($CDCl_3$): δ = 16.32 (2C, *C*H$_3$), 35.30 (2C, NCH$_2$*C*H$_2$NPht), 52.89 (d, $^3J_{CP}$=5.4 Hz, 2C, N*C*H$_2$CH$_2$NPht), 52.96 (d, $^1J_{CP}$=112 Hz, 1C, N*C*H$_2$P), 60.65 (d, $^2J_{CP}$=6.6 Hz, 2C, PO*C*H$_2$), 123.01, 132.04 and 133.75 (all Ph*t*), 128.39 (d, $^3J_{CP}$=12.1 Hz, 2C, *Ph*), 130.32 (d, $^1J_{CP}$=119 Hz, 1C, *Ph*), 131.76 (d, $^2J_{CP}$=9.4 Hz, 2C, *Ph*), 132.30 (1C, *Ph*), 167.97 (4C, *C*O); ^{31}P NMR ($CDCl_3$): δ = 40.18.

The material obtained was dissolved in dry ethanol (80 mL). Hydrazine hydrate (3.44 g, 68 mmol) was added, and the mixture was heated under reflux for 10 h. Precipitation of phthalhydrazide began after about 10 min of reflux. The mixture was cooled, and the phthalhydrazide formed was filtered off. The ethanol was evaporated, and water was removed by co-distillation with dry ethanol. The residue (intermediate (**10**)) was dissolved in DMF (80 mL). Then, $BrCH_2CO_2Et$ (36.7 g, 220 mmol, 8 equiv) and K_2CO_3 (30.4 g, 220 mmol) were added. The mixture was stirred at room temperature for 24 h. After filtering off the solids, the reaction mixture was diluted with a saturated aqueous solution of $NaHCO_3$ (50 mL), and the product was extracted into toluene (150 mL). The organic layer was washed with a saturated solution of $NaHCO_3$ (2×150 mL) and with brine (1×100 mL). The toluene phase was dried (Na_2SO_4), filtered and evaporated to dryness. NMR data of intermediate (**11**): ^{1}H NMR ($CDCl_3$): δ = 1.26 (m, 15H; CH_3), 2.73 (m, 8H; backbone CH_2), 3.10 (d, $^2J_{CP}$=10 Hz, 2H; NCH_2P), 3.48 (s, 8H; CH_2CO$_2$), 4.15 (m, 10H; OCH_2), 7.50, 7.84 (m, 5H; *Ph*); ^{31}P NMR ($CDCl_3$): δ = 40.48, and small impurities at ~20, 22, 35 and 40 ppm (<10%).

The crude intermediate (**11**) obtained above was dissolved in diluted HCl (250 mL, 1:1) and the mixture was heated under reflux for 18 h. During this time some precipitate formed. After cooling, the suspension was filtered, and nonpolar impurities were extracted with $CHCl_3$ (3×50 mL). Then, the aqueous phase was evaporated to dryness. The residue was dissolved in water and poured onto a cation-exchange column (Dowex 50, 170 mL, H^+ form). The nonbasic impurities were removed by elution with water. A yellow fraction containing the desired product was obtained by elution with a diluted ammonia (1:3) solution. This fraction was evaporated to dryness, redissolved in water and chromatographed on an anion exchanger (Dowex 1, 250 mL, OH^- form). After washing with water, some yellow-coloured impurities were removed with 10% acetic acid. The product was collected by elution with HCl (1:3). The solvents were evaporated off, and the product was dissolved in concentrated HCl (30 mL). Treatment with acetone (800 mL) gave a light yellow oil, which solidified upon standing. The white precipitate was filtered off, washed with acetone and dried at 80°C. Yield: 8.63 g (54%); m.p. 132–134°C (dec.); ^{1}H NMR (D_2O, pD 0.5): δ = 3.07 and 3.12 (10H; unresolved multiplets, NCH_2CH_2N and NCH_2P), 4.02 (s, 8H; NCH_2CO), 7.58, 7.63 and 7.80 (m, 5H; *Ph*); ^{13}C NMR (D_2O, pD 0.5): δ = 47.19 (d, $^3J_{CP}$=6.0 Hz,

2C, PCH_2NCH_2), 49.83 (2C, $PCH_2NCH_2CH_2N$), 52.10 (d, $^1J_{CP}=111$ Hz, 1C, NCH_2P), 56.69 (4C, NCH_2CO), 125.89 (d, $^3J_{CP}=12.1$ Hz, 2C, *Ph*), 128.57 (d, $^2J_{CP}=9.1$ Hz, 2C, *Ph*), 128.71 (1C, *Ph*), 133.03 (d, $^1J_{CP}=122$ Hz, 1C, *Ph*), 167.97 (4C, *CO*); ^{31}P NMR (D_2O, pD 0.5): δ = 31.63; ESI-MS: positive *m*/*z*: 490.3 $[M+H]^+$, negative *m*/*z*: 488.3 $[M-H]^-$; elemental analysis calcd (%) for $H_5L^2\cdot 2HCl\cdot H_2O$ ($C_{19}H_{32}Cl_2N_3O_{11}P$, *M* = 580.35; based on ^{1}H NMR, the product is slightly contaminated by acetone) C 39.32, H 5.56, Cl 12.22, N 7.24; found: C 39.82, H 5.43, Cl 11.50, N 7.17.

After evaporation of the mother liquor, a second crop of the product (1.02 g) was isolated in the same way.

Preparation of (*N*,*N*-dibenzylamino)methylphosphinic acid: Dibenzylamine (5.00 g, 25.3 mmol) was dissolved in ethanol (50 mL, 96%). Two equivalents of paraformaldehyde (1.52 g, 50.7 mmol) were added, and the mixture was heated to 60°C. Hypophosphorus acid (10.0 g of 50% aq. solution, 76.0 mmol) was added, and the reaction mixture was stirred at 60°C for 24 h. Then, chromatography on a strong cation exchanger in the H^+ form (Dowex 50, 200 mL, elution with water/ethanol 1:1 *v*/*v* and diluted ammonia), followed by chromatography on a strong anion exchanger (Dowex 1, 250 mL, acetate form, elution with water and 10% acetic acid), afforded the product as slightly yellow oil, which crystallised upon standing at room temperature. Yield: 6.30 g (85%); m.p. 66–68°C; ^{1}H NMR ($CDCl_3$): δ = 2.91 (d, $^2J_{PH}=7.2$ Hz, 2H; CH_2P), 4.27 (s, 4H; CH_2Ph), 7.31 (d, $^1J_{PH}=534$ Hz, 1H; *Ph*), 7.36 (m, 10H; *Ph*), 7.51 (m, 10H; *Ph*); ^{13}C NMR ($CDCl_3$): δ = 50.60 (d, $^1J_{PC}=84$ Hz, CH_2P), 58.36 (d, $^3J_{PC}=4.6$ Hz, NCH_2Ph), 129.04, 129.56, 129.73 and 131.37 (all *Ph*); ^{31}P NMR ($CDCl_3$): δ = 7.97 (dm, $^1J_{PH}=537$ Hz); ESI-MS: negative *m*/*z*: 274.1 $[M-H]^-$; elemental analysis calcd (%) for monohydrate ($C_{15}H_{20}NO_3P$, *M* = 293.30) C 61.43, H 6.87, N 4.78; found: C 61.24, H 6.69, N 4.96.

Preparation of ethyl (*N*,*N*-dibenzylamino)methylphosphinate: (*N*,*N*-dibenzylamino)methylphosphinic acid (3.03 g, 11.0 mmol) was suspended in chloroform (50 mL), and ethyl chloroformate (1.31 g, 12.1 mmol) was added. After 15 min, pyridine (0.96 g, 12.1 mmol) was added drop-wise (CO_2 was evolved immediately, the mixture remained heterogeneous). After 24 h at room temperature, a sample for ^{31}P NMR was filtered off. It showed only 65% conversion of acid to ester. Therefore, new portions of chloroformate (1 g) and pyridine (1.5 g) were added. After another 24 h, only one signal belonging to the desired ethyl ester was observed in the ^{31}P NMR spectrum (~35 ppm). The reaction mixture was washed with water (3×30 mL), dried (Na_2SO_4) and evaporated to dryness. The residue, a yellowish oil, was redissolved in toluene and evaporated in order to remove any excess of chloroformate. Yield: 3.30 g (99%); ^{1}H NMR ($CDCl_3$): δ = 1.34 (t, 3H; CH_3), 2.99 (m, 2H; NCH_2P), 3.78 (4H; AB-system, CH_2Ph), 4.07 (m, OCH_2), 6.97 (m, P-*H*, $^1J_{PH}=540$ Hz, 1H), 7.35 (m, 10H; *Ph*); ^{13}C NMR ($CDCl_3$): δ = 16.45 (d, $^3J_{CP}=6.0$ Hz, 1C, CH_3), 51.42 (d, $^1J_{CP}=114$ Hz, 1C, NCH_2P), 60.01 (d, $^3J_{CP}=7.7$ Hz, 2C, CH_2Ph), 62.45 (d, $^3J_{CP}=7.7$ Hz, 1C, OCH_2), 127.58 (2C), 128.58 (4C), 129.20 (4C) and 138.37 (2C; all Ph); ^{31}P NMR ($CDCl_3$): δ = 36.85 (dm, $^1J_{PH}=547$ Hz).

Preparation of diethylenetriamine-*N*′-methylene(dibenzylaminomethyl)-phosphinic-*N*,*N*,*N*″,*N*″-tetraacetic acid (H_5L^3): The freshly prepared ethyl (*N*,*N*-dibenzylamino)methylphosphinate (3.30 g, 10.9 mmol, 2 equiv) was dissolved with bis(phthaloyl)diethylenetriamine (**8**) (2.00 g, 5.5 mmol) in a mixture of toluene (50 mL) and ethanol (30 mL). The mixture was heated under reflux with a Dean–Stark trap. Over a period of 6 h, paraformaldehyde (0.50 g, 16.7 mmol, 3 equiv) was added in portions. The reaction mixture was refluxed overnight. An undecoupled ^{31}P NMR spectrum showed some unreacted P–H precursor (doublet at ~33 ppm) together with some phosphonic acid (~15 ppm) and two signals at ~48 ppm (probably the desired product (**9**) and hydroxymethyl(*N*,*N*-dibenzylamino)methylphosphinate). More paraformaldehyde was added, and the mixture was heated under reflux for another 12 h. During that time all of the P–H precursor disappeared. The reaction mixture was evaporated to dryness and re-dissolved in dry ethanol (40 mL). Hydrazine hydrate (0.83 g, 16.5 mmol, 3 equiv) was added, and the mixture was heated under reflux overnight. Precipitation of phthalhydrazide began after 10 min of reflux. The mixture was cooled, phthalhydrazide was filtered off, and the solvent was evaporated, yielding a yellowish oil. The product (**10**) was separated by chromatography on silica by using an aqueous ammonia/ethanol gradient (1:20 to 1:5). Yield 1.45 g (63%); ^{1}H NMR ($CDCl_3$): δ = 1.08 (br, 3H; CH_3), 1.75 (br, 4H), 2.45 (br, 8H), 2.50 (br, 8H), 2.68 (br, 8H), 3.60 (s, 4H; CH_2Ph), 4.00 (br, 2H; OCH_2), 7.10 (br, 10H; Ph); ^{13}C NMR ($CDCl_3$): δ = 16.98 (1C, CH_3), 39.82 (2C, CH_2Ph), 50.59 (d, $^1J_{CP}=113$ Hz, 1C, CH_2P), 51.99 (d, $^1J_{CP}=116$ Hz, 1C, CH_2P), 59.17 and 59.91 (2×2C, CH_2CH_2), 60.90 (d, $^2J_{CP}=7$ Hz, 1C, OCH_2), 127.45 (2C, Ph), 128.49 (4C, Ph), 129.35 (4C, Ph), 138.59 (2C, Ph); ^{31}P NMR ($CDCl_3$): δ = 49.69.

Compound (**10**) (5.90 g, 14.1 mmol) was stirred with $BrCH_2COOEt$ (11.8 g, 70 mmol) and K_2CO_3 (9.7 g, 70 mmol) in DMF (50 mL) at room temperature for 24 h. The reaction mixture was then extracted with toluene (100 mL), and the organic phase was extracted aqueous $NaHCO_3$ (3× 100 mL). After evaporation, a solution of NaOH (10 g) in water (50 mL) was added. Then, EtOH (≈50 mL) was added to obtain a homogeneous solution. This solution was stirred at room temperature for two days. The ^{31}P NMR spectrum showed that the reaction was complete (one major peak at 35.9 ppm). The reaction mixture was evaporated until dryness. The residue was dissolved in a minimum amount of water and then purified on a column of a strong cationic exchanger (Dowex 50, 150 mL, NH_4^+ form), with water (≈1000 mL) as the eluent. After elution, a ^{31}P NMR spectrum of the eluate was taken and showed the presence of H_5L^3. The fractions concerned were evaporated to obtain a yellow oil, which was crystallised at room temperature from an ethanol solution containing a small amount of acetone. The crystallisation started immediately. The product was filtered, washed with small amounts of ethanol and acetone, and dried at 80°C. Yield: 4.1 g (47%); m.p. 139–142°C (dec.); ^{1}H NMR (D_2O, pD 8.02): δ = 2.66 (dd, $^2J_{HP}=9.6$, 8.0 Hz, 4H; NCH_2PCH_2N), 2.85 (t, $^3J_{HH}=6.8$ Hz, 4H; NCH_2CH_2N), 3.07 (t, $^3J_{HH}=6.8$ Hz, 4H; NCH_2CH_2N), 3.58 (s, 8H; NCH_2COOH), 3.72 (s, 4H; NCH_2Ph), 7.33 (m, 10H; *Ph*), 7.40 (m, 10H; *Ph*); ^{13}C NMR (D_2O, pD 8.02): δ = 51.50 (d, $^3J_{CP}=5$ Hz, 2C, $NCH_2CH_2NCH_2CH_2N$), 53.06 (d, $^1J_{CP}=29.8$ Hz, 1C, $PCH_2NCH_2CH_2N$), 53.58 (d, $^1J_{CP}=75.5$ Hz, 1C, PCH_2NBn), 58.89 (2C, $NCH_2CH_2NCH_2COOH$), 60.63 (d, $^3J_{CP}=6.8$ Hz, 2C, NCH_2Ph), 71.34 (4C, NCH_2COOH), 129.18 (*Ph*), 130.18 (*Ph*), 131.65 (*Ph*), 139.73 (*Ph*), 174.14 (4C, CO); ^{31}P NMR (D_2O, pD 8.02): δ = 34.54; elemental analysis calcd (%) for $H_5L^3\cdot 2NH_3\cdot 0.5H_2O$ ($C_{28}H_{46}N_6O_{10.5}P$, *M* = 565.68) C 50.52, H 6.97, N 12.62; found: C 50.38, H 6.69, N 12.68; ESI-MS: positive *m*/*z*: 623.4 $[M+H]^+$; negative *m*/*z*: 621.7 $[M-H]^-$.

pH Dependence of ^{1}H and ^{31}P NMR spectra: For these experiments, 0.1 M solutions of ligands H_6L^1 and H_5L^2 in H_2O/D_2O (9:1) and H_5L^3 and $[La(L^3)(H_2O)]^{2-}$ in D_2O were prepared. The pH was adjusted by stepwise addition of a solution of NaOH or HCl (both prepared in H_2O/D_2O (9:1) for H_6L^1 and H_5L^2 and in pure D_2O for H_5L^3 and $[La(L^3)(H_2O)]^{2-}$). The pH values reported for H_5L^3 were corrected for the deuterium effect by using the relationship pD = pH + 0.4.[54] A drop of *t*BuOH (δ = 1.2 ppm) was added to the samples as internal reference for ^{1}H. The assignment of the backbone hydrogen atoms was done by using selective ^{1}H-decoupled ^{13}C NMR spectroscopy for the free ligands and COSY spectra for $[La(L^3)(H_2O)]^{2-}$. The calculations were performed by using the computer programs Micromath Scientist, version 2.0 (Salt Lake City, UT, USA) or OPIUM.[55] Both of them resulted in the same values of pK_a (within standard errors).

Analysis of induced shifts in ^{17}O NMR spectra of lanthanide(III) complexes: Samples with a complex concentration of about 0.2 M were prepared. The solid lanthanide(III) chlorides and solid ligands (~10% excess) were dissolved in a weighed amount of D_2O in a small vial containing a stirring bar and a microscopic grain of methyl red indicator. The vials were capped with a septum, and then a solution of 10–15% sodium hydroxide in D_2O was added dropwise from a syringe with stirring till a colour change of the indicator (pH~4–6). Then the vial was weighed again. From the increase of the weight, the molar ratio of exchangeable oxygen atoms per Ln^{3+} ion was calculated.

Relaxation enhancements in ^{13}C and ^{31}P NMR spectra of lanthanide(III) complexes: For these experiments, the samples prepared for ^{17}O NMR experiments described above were used. The longitudinal relaxation rates were measured at 80°C by using the inversion-recovery method.[56]

Variable temperature ^{17}O NMR study of Gd^{3+} complexes: Solutions of Gd^{3+} complexes of H_6L^1, H_5L^2 and H_5L^3 with a concentration of about 0.15 M were prepared by dissolution of exactly weighed solid $GdCl_3\cdot 6H_2O$ and the solid ligands (H_6L^1 and H_5L^2 as the hydrochloride salts, ~10%

excess) in a weighed amount of deionised water. Calculated amounts of sodium hydroxide (9 and 8 equivalents for H_6L^1 and H_5L^2 or H_5L^3, respectively, as 10% solution) were added dropwise with stirring. After the mixture had stood for 30 min at room temperature, the pH was checked. All samples gave a negative Xylenol orange test for the presence of free Gd^{3+}. All NMR spectra were conducted without a frequency lock. To correct the ^{17}O NMR shift for the contribution of the bulk magnetic susceptibility (BMS), the difference between chemical shifts of proton signals of acetone (or *tert*-butanol) in the paramagnetic sample and in pure water was used.[57] Longitudinal ($1/T_1$) and transversal ($1/T_2$) relaxation rates were obtained by the inversion-recovery method[56] and the Carr–-Purcell–Meiboom–Gil pulse sequence,[58] respectively. Experimental data were fitted with a computer program written by Dr. É. Tóth and Dr. L. Helm (EPFL Lausanne, Switzerland) using the Micromath Scientist program, version 2.0 (Salt Lake City, UT, USA).

Concentration dependence of ^2H NMR longitudinal-relaxation time: Deuterium-containing ligands were prepared by H–D exchange from H_6L^1, H_5L^2 and H_5L^3 in D_2O/K_2CO_3 (pD 10.5) by heating mixtures at 95°C for 5 d, analogously to the method reported in the literature.[31] The ligand and $LaCl_3{\cdot}7H_2O$ (equivalent amounts) were dissolved in deuterium-depleted water (1 mL). Then the pH was adjusted to a value close to neutral by addition of small portions of solid $LiOH{\cdot}H_2O$. The transversal-relaxation rates were measured by using the inversion-recovery pulse sequence.

EPR Measurements: EPR spectra of the Ln^{III} complexes in aqueous solution were recorded on a Bruker ESP300E spectrometer operating at 9.43 GHz (0.34 T, X-band). 5 mM aqueous solutions of the complexes were measured at 298 K in a quartz flat cell. Typical parameters used were: sweep width 40 mT, microwave power 20 mW, modulation amplitude 0.32 mT and time constant 0.02 s. The frequency was calibrated with diphenylpicrylhydrazyl (dpph) and the magnetic field with Mn^{2+} in MgO.

Measurements of NMRD profiles: The samples were prepared by mixing the ligand under study with a slight excess of solid $GdCl_3{\cdot}6H_2O$, followed by dissolution in water. The pH values of the solutions were adjusted to about 7 with a NaOH solution. The solutions were then stirred overnight in the presence of Chelex 20 to remove the remaining free Gd^{3+}. The solids were removed in a centrifuge, and the remaining solutions were freeze-dried. The solid complexes were dissolved in an appropriate amount of water. The absence of free Gd^{3+} was checked with an Arsenazo III indicator. The concentrations of Gd^{3+} in the samples were determined from proton-relaxivity measurements at 20 MHz and 37°C after complete hydrolysis. The purity of complex solutions was checked by ESI-MS; $[Gd(L^1)]^{3-}$: m/z: 651 $[M+3Na]^+$, 673 $[M+4Na]^+$, 695 $[M+5Na]^+$, 730 $[M+5Na+K]^+$; $[Gd(L^2)]^{2-}$: m/z: 711 $[M+3Na]^+$, 769 $[M+2Na+K]^+$; $[Gd(L^3)]^{2-}$: m/z: 822 $[M+2Na]^+$; 844 $[M+3Na]^+$.

The complexes $[Gd(L^1)(H_2O)]^{3-}$, $[Gd(L^2)(H_2O)]^{2-}$ and $[Gd(L^3)(H_2O)]^{2-}$ were studied by ^1H longitudinal-relaxation-time measurements. NMRD profiles were measured at 5, 25 and 37°C at magnetic field strengths between 4.7×10^{-4} and 0.35 T (Stelar SpinMaster FFC-2000). Measurements at 0.47, 1.42 and 7.05 T were performed on Bruker Minispec 20 and 60 MHz and on a Bruker AMX-300 spectrometer (Bruker, Karlsruhe, Germany), and were included in the profiles. The experimental data were fitted simultaneously with ^{17}O NMR data, ^1H NMRD data and data obtained from the temperature dependence of relaxivity at constant magnetic field (20 MHz), by using a least-squares fitting procedure with the Micromath Scientist program version 2.0 (Salt Lake City, UT, USA).

Interaction of $[Gd(L^3)(H_2O)]^{2-}$ with HSA: For human serum albumin interaction studies, a stock solution of $[Gd(L^3)(H_2O)]^{2-}$ in water was prepared as described in the preceding section. The dependence of the proton-relaxation rate on the concentration of the Gd^{3+} complex at constant HSA concentration (4%) was measured by using a Minispec PC-20 at a constant magnetic field of 0.47 T and a constant temperature of 310 K. The concentrations of $[Gd(L^3)(H_2O)]^{2-}$ varied from 0.038 to 0.81 mM. Longitudinal-relaxation rates of the solution containing 4% HSA and 0.81 mM complex were measured at 310 K over the range of magnetic fields 4×10^{-4}–7.05 T.

Transmetallation experiments: The stability of Gd^{3+} complexes was determined by transmetallation with $ZnCl_2$. These measurements were done by using a buffered solution (phosphate buffer, total concentration 67 mM, pH 7) containing of Gd^{3+} complex (2.5 mM) and $ZnCl_2$ (2.5 mM). The transmetallation was followed by the ^1H longitudinal-relaxation rates of the water at Bruker Minispec 20 MHz (Bruker, Karlsruhe, Germany) at 37°C.

Acknowledgement

This work was performed within the framework of the EU COST Action D18: Lanthanide chemistry for diagnosis and therapy. Thanks are due to the EU for financial support through a Marie Curie training site host fellowship (QLK5-CT-2000-60062) and to Kristina Djanashvili for some NMR measurements. The work was supported by the Grant Agency of the Czech Republic (203/02/0493 and 203/03/0168). J.K. thanks the Charles University Grant Agency (250/2003/B-Ch).

[1] *The Chemistry of Contrast Agents in Medical Magnetic Resonance Imaging* (Eds.: A. E. Merbach, É. Tóth), Wiley, Chichester, **2001**.
[2] P. Caravan, J. J. Ellison, T. J. McMurry, R. B. Lauffer, *Chem. Rev.* **1999**, *99*, 2293.
[3] S. Liu, D. S. Edwards, *Bioconjugate Chem.* **2001**, *12*, 7.
[4] R. B. Lauffer, *Chem. Rev.* **1987**, *87*, 901.
[5] V. Jacques, J. F. Desreux, *Top. Curr. Chem.* **2002**, *221*, 123.
[6] S. Aime, M. Botta, M. Fasano, E. Terreno, *Chem. Soc. Rev.* **1998**, *27*, 19.
[7] I. Lukeš, P. Cígler, J. Kotek, J. Rudovský, P. Hermann, J. Rohovec, P. Vojtíšek, *J. Inorg. Biochem.* **2001**, *86*, 68.
[8] S. Aime, M. Botta, S. G. Crich, G. Giovenzana, R. Pagliarin, M. Sisti, E. Terreno, *Magn. Reson. Chem.* **1998**, *36*, S200.
[9] S. Aime, M. Botta, L. Frullano, S. G. Crich, G. Giovenzana, R. Pagliarin, G. Palmisano, F. R. Sirtori, M. Sisti, *J. Med. Chem.* **2000**, *43*, 4017.
[10] D. J. Parmelee, R. C. Walovitch, H. S. Ouellet, R. B. Lauffer, *Invest. Radiol.* **1997**, *32*, 741.
[11] G. R. Choppin, P. A. Bertand, Y. Hasegawa, E. N. Rizkalla, *Inorg. Chem.* **1982**, *21*, 3722.
[12] G. R. Choppin, *J. Less-Common Met.* **1985**, *112*, 193.
[13] I. Lukeš, J. Kotek, P. Vojtíšek, P. Hermann, *Coord. Chem. Rev.* **2001**, *216–217*, 287, and references therein.
[14] J. L. Sudmeier, C. N. Reilley, *Anal. Chem.* **1964**, *9*, 1698.
[15] C. F. G. C. Geraldes, A. M. Urbano, M. C. Alpoim, A. D. Sherry, K.-T. Kuan, R. Rajagopalan, F. Maton, R. N. Muller, *Magn. Reson. Imaging* **1995**, *13*, 401.
[16] E. N. Rizkalla, G. R. Choppin, *Inorg. Chem.*, **1983**, *22*, 1478.
[17] C. F. G. C. Geraldes, A. D. Sherry, W. P. Cacheris, *Inorg. Chem.* **1989**, *28*, 3336.
[18] R. M. Smith, A. E. Martell, *Critical Stability Constants, Vols. 1–6*, Plenum, New York, **1974–1989**.
[19] K. Sawada, T. Araki, T. Suzuki, *Inorg. Chem.* **1987**, *26*, 1199.
[20] J. A. Peters, J. Huskens, D. J. Raber, *Prog. Nucl. Magn. Reson. Spectrosc.* **1996**, *28*, 283, and references therein.
[21] R. M. Golding, M. P. Halton, *Aust. J. Chem.* **1972**, *25*, 2577.
[22] A. A. Pinkerton, M. Rossier, S. Spiliadis, *J. Magn. Reson.* **1985**, *64*, 420.
[23] B. Bleaney, *J. Magn. Reson.* **1972**, *8*, 91.
[24] B. Bleaney, C. M. Dobson, B. A. Levine, R. B. Martin, R. J. P. Williams, A. V. Xavier, *Chem. Commun.* **1972**, 791.
[25] R. M. Golding, P. Pyykkö, *Mol. Phys.* **1973**, *6*, 1389.
[26] J. A. Peters, *Inorg. Chem.* **1988**, *27*, 4686.
[27] J. A. Peters, *J. Magn. Reson.* **1985**, *65*, 417.
[28] C. Platas, F. Avecilla, A. de Blas, C. F. G. C. Geraldes, T. Rodríguez-Blas, H. Adams, J. Mahía, *Inorg. Chem.* **1999**, *38*, 3190.
[29] B. M. Alsaadi, F. J. C. Rossotti, R. J. P. Williams, *J. Chem. Soc. Dalton Trans.* **1980**, 2147.
[30] C. F. G. C. Geraldes, A. M. Urbano, M. A. Hoefnagel, J. A. Peters, *Inorg. Chem.* **1993**, *32*, 2426.
[31] H. Lammers, F. Maton, D. Pubanz, M. W. van Laren, H. van Bekkum, A. E. Merbach, R. N. Muller, J. A. Peters, *Inorg. Chem.* **1997**, *36*, 2527.

[32] J. A. Peters, E. Zitha-Bovens, D. M. Corsi, C. F. G. C. Geraldes in *The Chemistry of Contrast Agents in Medical Magnetic Resonance Imaging* (Eds.: A. E. Merbach, É. Tóth), Wiley, Chichester, **2001**, p. 315.
[33] L. Frullano, J. Rohovec, J. A. Peters, C. F. G. C. Geraldes, *Top. Curr. Chem.* **2002**, *211*, 25.
[34] L. Vander Elst, S. Laurent, R. N. Muller, *Invest. Radiol.* **1998**, *33*, 828.
[35] É. Tóth, L. Helm, A. E. Merbach in *The Chemistry of Contrast Agents in Medical Magnetic Resonance Imaging* (Eds.: A. E. Merbach, É. Tóth), Wiley, Chichester, **2001**, p. 45.
[36] D. H. Powell, O. M. N. Dhubhghaill, D. Pubanz, L. Helm, Y. S. Lebedev, W. Schlaepfer, A. E. Merbach, *J. Am. Chem. Soc.* **1996**, *118*, 9333.
[37] F. A. Dunand, A. Borel, A. E. Merbach, *J. Am. Chem. Soc.* **2002**, *124*, 710.
[38] J. C. Hindman, *J. Chem. Phys.* **1973**, *60*, 4488.
[39] M. Botta, *Eur. J. Inorg. Chem.* **2000**, 399.
[40] S. Aime, M. Botta, L. Frullano, S. Geninatti Crich, G. Giovenzana, R. Pagliarin, G. Palmisano, F. R. Sirtori, M. Sisti, *J. Med. Chem.* **2000**, *43*, 4017.
[41] K. I. Hardcastle, M. Botta, M. Fasano, G. Digilio, *Eur. J. Inorg. Chem.* **2000**, 971.
[42] S. Aime, M. Botta, S. Geninatti Crich, E. Terreno, *J. Biol. Inorg. Chem.* **1997**, *2*, 470.
[43] J. Reuben, *J. Chem. Phys.* **1971**, *75*, 3164.
[44] A. Borel, É. Tóth, L. Helm, A. Janóssy, A. E. Merbach, *Phys. Chem. Chem. Phys.* **2000**, *2*, 1311.
[45] L. Burai, É. Tóth, G. Moreau, A. Sour, R. Scopelliti, A. E. Merbach, *Chem. Eur. J.* **2003**, *9*, 1394.
[46] S. Rast, A. Borel, L. Helm, E. Belorizky, P. H. Fries, A. E. Merbach, *J. Am. Chem. Soc.* **2001**, *123*, 2637.
[47] S. Aime, M. Chiaussa, G. Digilio, E. Gianolio, E. Terreno, *J. Biol. Inorg. Chem.* **1999**, *4*, 766.
[48] R. N. Muller, B. Radüchel, S. Laurent, J. Platzek, C. Piérart, P. Mareski, L. Vander Elst, *Eur. J. Inorg. Chem.* **1999**, 1949.
[49] S. Laurent, L. Vander Elst, F. Copoix, R. N. Muller, *Invest. Radiol.* **2001**, *36*, 115.
[50] C. Y. Ng, R. J. Motekaitis, A. E. Martell, *Inorg. Chem.* **1979**, *18*, 2982.
[51] D. B. Hope, K. C. Horncastle, *J. Chem. Soc. C* **1966**, 1098.
[52] A. E. Martin, T. M. Ford, J. E. Bulkowski, *J. Org. Chem.* **1982**, *47*, 412.
[53] D. G. Hewitt, *Aust. J. Chem.* **1979**, *32*, 463.
[54] D. K. Lavallee, A. H. Zeltmann, *J. Am. Chem. Soc.* **1974**, *96*, 5552.
[55] OPIUM program package: M. Kývala, I. Lukeš, CHEMOMETRICS'95, Pardubice, Czech Republic, **1995**, Book of Abstracts p. 63, OPIUM program package: M. Kývala, P. Lubal, I. Lukeš, SIMEC'98, Girona, Spain, **1998**, Book of Abstracts p. 94; available free of charge at: http://www.natur.cuni.cz/~kyvala/opium.html
[56] R. L. Vold, J. S. Waugh, M. P. Klein, D. E. Phelps, *J. Chem. Phys.* **1968**, *48*, 3831.
[57] E. Zitha-Bovens, L. V. Elst, R. N. Muller, H. van Bekkum, J. A. Peters, *Eur. J. Inorg. Chem.* **2001**, 3101.
[58] S. Meiboom, D. Gill, *Rev. Sci. Instrum.* **1958**, *29*, 688.

Received: May 19, 2003 [F5155]

